Power corrections in charmless nonleptonic B decays: Annihilation is factorizable and real

Christian M. Arnesen,[1] Zoltan Ligeti,[1,2] Ira Z. Rothstein,[3] and Iain W. Stewart[1]

[1]*Center for Theoretical Physics, Laboratory for Nuclear Science, Massachusetts Institute of Technology, Cambridge, Massachusetts 02139, USA*

[2]*Ernest Orlando Lawrence Berkeley National Laboratory, University of California, Berkeley, California 94720, USA*

[3]*Department of Physics, Carnegie Mellon University, Pittsburgh, Pennsylvania 15213, USA*

(Received 17 July 2006; published 6 March 2008)

We classify $\Lambda_{\rm QCD}/m_b$ power corrections to nonleptonic $B \to M_1 M_2$ decays, where $M_{1,2}$ are charmless nonisosinglet mesons. Using recent developments in soft-collinear effective theory, we prove that the leading contributions to annihilation amplitudes of order $\alpha_s(m_b)\Lambda_{\rm QCD}/m_b$ are real. The leading annihilation amplitudes depend on twist-2 and twist-3 three-parton distributions. A complex nonperturbative parameter from annihilation first appears at $\mathcal{O}[\alpha_s^2(\sqrt{\Lambda m_b})\Lambda_{\rm QCD}/m_b]$. "Chirally enhanced" contributions are also factorizable and real at lowest order. Thus, incalculable strong phases are suppressed in annihilation amplitudes, unless the $\alpha_s(\sqrt{\Lambda m_b})$ expansion breaks down. Modeling the distribution functions, we find that $(11 \pm 9)\%$ and $(15 \pm 11)\%$ of the absolute values of the measured $\bar{B}^0 \to K^- \pi^+$ and $B^- \to K^- K^0$ penguin amplitudes come from annihilation. This is consistent with the expected size of power corrections.

DOI: 10.1103/PhysRevD.77.054006 PACS numbers: 13.25.Hw, 12.39.St

I. INTRODUCTION

Nonleptonic charmless B decays are important probes of the standard model (SM). They are sensitive to the CP violating phase γ (or α) via the interference of tree and penguin contributions, and to possible new physics that could modify the penguin amplitudes. They also provide a powerful laboratory to study strong interactions, the understanding of which is crucial if one is to claim sensitivity to new physics in these decays.

The theory of nonleptonic B decays underwent important progress in the last few years. Factorization theorems for $B \to MM'$ decays have been proven to all orders in α_s at leading order in Λ/m_b, for decays when M is a light (charmless) meson and M' is either charmed or charmless [1–5]. Here $\Lambda \sim \Lambda_{\rm QCD} \sim 500$ MeV denotes a typical hadronic scale. An important difference between the various approaches to making predictions for the charmless $B \to M_1 M_2$ decay rates [2,5–13] is how certain $\mathcal{O}(\Lambda/m_b)$ power suppressed corrections are treated. In particular, it was observed that so-called annihilation diagrams (as in Fig. 2) give rise to divergent convolution integrals if one attempts calculating them using conventional factorization techniques [7]. In the KLS, or perturbative QCD (pQCD), approach [7], these are rendered finite by $k_\perp$ dependences, which effectively cut off the endpoints of the meson distribution functions. KLS found large imaginary parts from the jet scale, $\sqrt{m_b\Lambda}$, from propagators via $\mathrm{Im}[xm_b^2 - k_\perp^2 + i\epsilon]^{-1} = -\pi\delta(xm_b^2 - k_\perp^2)$ [14]. They also found that for the physical value of m_b the power suppression of these terms relative to the leading contributions was not very significant. In the BBNS, or QCD factorization (QCDF), approach [2,10,11], the divergent convolutions are interpreted as signs of infrared sensitive contributions, and are modeled by complex parameters, $X_A = \int_0^1 dy/y = (1 + \rho_A e^{i\varphi_A}) \ln(m_B/\Lambda)$, with $\rho_A \leq 1$ and an unrestricted strong phase φ_A. In Ref. [15] annihilation diagrams were investigated in the soft-collinear effective theory (SCET) [16] and parametrized by a complex amplitude. When annihilation is considered in $SU(3)$ flavor analyses, a complex parameter is also used [17]. In the absence of a factorization theorem for annihilation contributions, a dimensional analysis based parametrization with Λ/m_b magnitude and unrestricted strong phases is a reasonable way of estimating the uncertainty. In order not to introduce model dependent correlations, a new parameter could be used for each independent channel.

It was recently shown by Manohar and Stewart [18] that properly separating the physics at different momentum scales removes the divergences, giving well-defined results for convolution integrals through a new type of factorization that separates modes by their invariant mass and rapidity. The analysis involves a minimal subtraction with the zero-bin method to avoid double counting rapidity regions, and with the regulation and subtraction of divergences for large p^+ and p^- momenta that behave like ultraviolet divergences. Additional subtractions would correspond to scheme dependent terms, so the minimal subtraction is the usual and simplest choice. We refer to this as MS factorization.[1] In this paper we classify annihilation contributions to $B \to M_1 M_2$ decays and demonstrate how this rapidity factorization works for the leading terms of order $\alpha_s(m_b)\Lambda/m_b$. These leading order annihilation contributions are real despite the presence of endpoint divergences. We also classify which terms can involve a nonperturbative complex hadronic parameter, and show that they first show up for annihilation at higher order in perturbation theory, $\mathcal{O}[\alpha_s^2(\sqrt{m_b\Lambda})\Lambda/m_b]$.

[1]Over the objection of one of the authors.

Our analysis demonstrates that, while certain annihilation contributions are only sensitive to the hard short-distance scale $\mu^2 \sim m_b^2$ (local annihilation), there exist other annihilation contributions that start at the same order in α_s and $1/m_b$ and are sensitive to the intermediate scale $\mu^2 \sim m_b\Lambda$ (hard-collinear annihilation terms). The leading local annihilation terms involve f_B and a modified type of twist-2 distribution functions, while the leading hard-collinear terms have twist-3 meson distributions. In this work we perform matching calculations for the two-body distributions that require rapidity factorization. The calculation of the leading amplitude involving the three-body functions is given in a separate publication [19]; however, we review the numerical results here.

An interesting set of power corrections are those proportional to μ_P, where $\mu_\pi = m_\pi^2/(m_u + m_d)$ and $\mu_K = m_K^2/(m_u + m_s)$ [20]. For kaons and pions $\mu_P \sim 2$ GeV, so corrections proportional to μ_P/m_b can be sizable, and were labeled "chirally enhanced" in Refs. [2,10]. In the chiral limit $\mu_P \propto \Lambda_\chi$, where Λ_χ is the chiral symmetry breaking scale, so the enhancement is not parametric, and comes from the fact that $\Lambda_\chi > \Lambda_{\rm QCD}$. In the BBNS approach these Λ^2/m_b^2 annihilation power corrections are included along with the leading order terms, and when they multiply divergent convolutions they are described by complex parameters. Below we show that, much like the lowest order annihilation contributions, these terms are also real and factorizable.

In Sec. II we review the leading order factorization theorem, and classify power corrections to $B \to M_1M_2$, with a focus on annihilation amplitudes. In Sec. III a factorization theorem is derived for local annihilation amplitudes at order Λ/m_b for final states not involving isosinglets [given in Eq. (23)]. These amplitudes start at $\mathcal{O}(\alpha_s(m_b))$ and involve f_B and a modified type of twist-2 meson distributions. The extension to chirally enhanced local annihilation terms is considered in Sec. IV. In Sec. V we study annihilation amplitudes from time-ordered products, and classify complex contributions generated at the hard scale m_b, the intermediate scale $\sqrt{m_b\Lambda}$, and the nonperturbative scale Λ. Our results give absolute predictions for the annihilation amplitudes in $B \to PP, PV, VV$ channels, given the meson distribution functions as inputs, which are studied in Sec. VI. This section also discusses the implications of our results for models of annihilation used in the literature, and a numerical analysis of the annihilation amplitudes in $\bar B \to K\pi$ and $\bar B \to K\bar K$. The Appendix gives the derivation of a two-dimensional convolution formula with overlapping zero-bin subtractions.

II. ANNIHILATION CONTRIBUTIONS IN SCET

We use M to denote a charmless pseudoscalar or vector meson ($\pi, K, \rho, \ldots$). The relevant scales in $B \to M_1M_2$ decays are m_W, m_b, $E \approx m_B/2$, m_c, the jet scale $\sqrt{E\Lambda}$, and the nonperturbative scale Λ. Here E is the energy of the light mesons, which is much greater than their masses, $m_{M_{1,2}} \sim \Lambda$. To simplify notation, we denote by m_b hereafter the expansion in all hard scales, $\{m_b, E, m_c\}$. The decays $B \to M_1M_2$ are mediated by the weak $\Delta B = 1$ effective Hamiltonian, which has $\Delta S = 0$ terms for $\bar b \to \bar d q_1 \bar q_2$ transitions and $\Delta S = 1$ terms for $\bar b \to \bar s q_1 \bar q_2$. For $\Delta S = 0$ it reads

$$H_W = \frac{G_F}{\sqrt{2}} \sum_{p=u,c} V_{pb}V_{pd}^* \Big(C_1 O_1^p + C_2 O_2^p + \sum_{i=3}^{10,7\gamma,8g} C_i O_i \Big), \tag{1}$$

where the operators are

$$\begin{aligned}
O_1^u &= (\bar u b)_{V-A}(\bar d u)_{V-A},\\
O_2^u &= (\bar u_\beta b_\alpha)_{V-A}(\bar d_\alpha u_\beta)_{V-A},\\
O_1^c &= (\bar c b)_{V-A}(\bar d c)_{V-A},\\
O_2^c &= (\bar c_\beta b_\alpha)_{V-A}(\bar d_\alpha c_\beta)_{V-A},\\
O_3 &= \sum_{q'} (\bar d b)_{V-A}(\bar q' q')_{V-A},\\
O_4 &= \sum_{q'} (\bar d_\beta b_\alpha)_{V-A}(\bar q'_\alpha q'_\beta)_{V-A},\\
O_5 &= \sum_{q'} (\bar d b)_{V-A}(\bar q' q')_{V+A},\\
O_6 &= \sum_{q'} (\bar d_\beta b_\alpha)_{V-A}(\bar q'_\alpha q'_\beta)_{V+A},\\
O_7 &= \sum_{q'} \frac{3e_{q'}}{2} (\bar d b)_{V-A}(\bar q' q')_{V+A},\\
O_8 &= \sum_{q'} \frac{3e_{q'}}{2} (\bar d_\beta b_\alpha)_{V-A}(\bar q'_\alpha q'_\beta)_{V+A},\\
O_9 &= \sum_{q'} \frac{3e_{q'}}{2} (\bar d b)_{V-A}(\bar q' q')_{V-A},\\
O_{10} &= \sum_{q'} \frac{3e_{q'}}{2} (\bar d_\beta b_\alpha)_{V-A}(\bar q'_\alpha q'_\beta)_{V-A},\\
O_{7\gamma} &= -\frac{e}{8\pi^2} m_b \bar d \sigma^{\mu\nu} F_{\mu\nu}(1+\gamma_5) b,\\
O_{8g} &= -\frac{g}{8\pi^2} m_b \bar d \sigma^{\mu\nu} G^a_{\mu\nu} T^a (1+\gamma_5) b.
\end{aligned} \tag{2}$$

Here $O_{1,2}^u$ and $O_{1,2}^c$ are current-current operators, α and β are color indices, O_{3-6} are penguin operators, and O_{7-10} are electroweak penguin operators, with a sum over $q' = u, d, s, c, b$ flavors, and electric charges $e_{q'}$. Results for $\Delta S = 1$ transitions are obtained by replacing $d \to s$ in Eqs. (1) and (2), and likewise in the equations below. The coefficients in Eq. (1) are known at next-to-leading-log (NLL) order [21] (we have $O_1^p \leftrightarrow O_2^p$ relative to [21]). In the naive dimensional regularization (NDR) scheme,

taking $\alpha_s(m_Z) = 0.118$ and $m_b = 4.8$ GeV,

$$C_{1-10}(m_b) = \{1.080,\ -0.177,\ 0.011,\ -0.033,\ 0.010,\ -0.040,\ 4.9\times10^{-4},\ 4.6\times10^{-4},\ -9.8\times10^{-3},\ 1.9\times10^{-3}\}. \quad (3)$$

To define what we mean by annihilation amplitudes we use the contraction amplitudes $A_1, A_2, P_3, P_3^{\rm GIM}$ in the full electroweak theory from Ref. [22] (which thus includes penguin annihilation). These amplitudes are scheme and scale independent and correspond to Feynman diagrams with a Wick contraction between the spectator flavor in the initial state and a quark in the operators O_i. Using SCET these annihilation amplitudes can be proven to be suppressed by Λ/m_b to all orders in α_s [5]. These contributions differ from emission-annihilation amplitudes, EA_1 and EA_2, which involve at least one isosinglet meson. As demonstrated in Refs. [11,23], $EA_{1,2}$ occur at leading order in the power expansion. We focus on isodoublet and isotriplet final states, so ignore the $EA_{1,2}$ amplitudes hereafter.

To separate the mass scales occurring below m_b, we need to match H_W onto operators in SCET. The nonperturbative degrees of freedom are soft quarks and gluons for the B meson, n-collinear quarks and gluons for one light meson, and $\bar n$-collinear fields for the other light meson, as defined in [24]. Expanding in Λ/m_b gives

$$\begin{aligned}\langle M_1M_2|H_W|B\rangle &= A^{(0)} + A_{c\bar c} + A^{(1)}_{\rm ann} + A^{(1)}_{\rm rest} + \ldots \\ &= \frac{G_F m_B f_{M_1} f_{M_2} f_B}{\sqrt{2}\Lambda_0}[\hat A^{(0)} + \hat A_{c\bar c} + \hat A^{(1)}_{\rm ann} \\ &\quad + \hat A^{(1)}_{\rm rest} + \ldots]. \end{aligned} \quad (4)$$

In the second and third lines we switched to dimensionless amplitudes $\hat A$ by pulling out a prefactor with the correct $\Lambda^{5/2}m_b^{1/2}$ scaling. Here $\Lambda_0 = 500$ MeV represents a B-meson scale that is $\mathcal{O}(\Lambda_{\rm QCD})$. Taking $\eta = \Lambda/m_b$ we have the leading order amplitude $\hat A^{(0)} = \mathcal{O}(\eta^0)$, and the subleading amplitude $\hat A^{(1)} = \hat A^{(1)}_{\rm ann} + \hat A^{(1)}_{\rm rest} = \mathcal{O}(\eta^1)$, which we have split into the annihilation amplitude $\hat A^{(1)}_{\rm ann}$ and the remainder $\hat A^{(1)}_{\rm rest}$. The amplitude $\hat A_{c\bar c}$ in Eq. (4) denotes contributions from long-distance charm effects in all amplitudes, while perturbative charm loops contribute in the amplitudes $A^{(0)}$ and $A^{(1)}$.[2]

There are two formally large scales, $m_b \gg \sqrt{m_b\Lambda} \gg \Lambda$, which we will refer to as the hard scale $\mu_h \sim m_b$, and intermediate or hard-collinear scale $\mu_i \sim \sqrt{m_b\Lambda}$. These scales can be integrated out one by one [27] with effective theories SCET$_{\rm I}$ and SCET$_{\rm II}$. Integrating out m_b requires matching the O_i onto a series of operators in SCET$_{\rm I}$, $Q^{(j)} \sim \lambda^j$ where the SCET$_{\rm I}$ power counting parameter $\lambda = \eta^{1/2} = \sqrt{\Lambda/m_b}$. To obtain contributions to $B \to M_1M_2$, we require an odd number of ultrasoft (usoft) light quarks $q_{\rm us}$, two or more n-collinear fields, and two or more $\bar n$-collinear fields, where $n^2 = \bar n^2 = 0$.

We briefly review results from Refs. [4,5] for the leading amplitude $A^{(0)}$ for $B \to M_1M_2$. Here we have weak operators $Q^{(0)}_{1d-6d} \sim \lambda^6$, $Q^{(1)}_{1d-8d} \sim \lambda^7$ with no $q_{\rm us}$'s, taken in time-ordered products with a usoft-collinear quark Lagrangian, $\mathcal{L}^{(j)}_{\xi q} \sim \lambda^j$ for $j = 1, 2$, which has one $q_{\rm us}$. We denote other subleading Lagrangians by $\mathcal{L}^{(j)}$, and list the $\mathcal{O}(\lambda^7)$ and $\mathcal{O}(\lambda^8)$ time-ordered products for $A^{(0)}$ in Table I. Matching these time-ordered products onto SCET$_{\rm II}$ gives the leading $\mathcal{O}(\eta^6)$ operators.[3] When combined with the $\eta^{-7/2}$ from the states this yields a matrix element of order $\eta^{5/2}$, in agreement with the prefactor in Eq. (4). Examples of the weak operators in SCET$_{\rm I}$ are

$$\begin{aligned} Q^{(0)}_{1d} &= [\bar u_{n,\omega_1} \not{\bar n} P_L b_v][\bar d_{\bar n,\omega_2} \not{n} P_L u_{\bar n,\omega_3}], \\ Q^{(1)}_{1d} &= [\bar u_{n,\omega_1} ig \not{\mathcal{B}}^\perp_{n,\omega_4} P_L b_v][\bar d_{\bar n,\omega_2} \not{n} P_L u_{\bar n,\omega_3}], \end{aligned} \quad (5)$$

where other $Q^{(0,1)}_{id}$ have different flavor structures. The "quark" fields with subscripts n and $\bar n$ contain a collinear quark field and Wilson line with large momenta labels ω_i, such as

$$\bar u_{n,\omega} = [\bar\xi^{(u)}_n W_n \delta(\omega - \bar n\cdot\mathcal{P}^\dagger)]. \quad (6)$$

Here $\bar\xi_n$ creates an n-collinear quark, or annihilates an antiquark, $W_n = W[\bar n\cdot A_n]$ is the standard SCET collinear Wilson line built from the $\bar n$ component of n-collinear gluons, $\bar n\cdot\mathcal{P}^\dagger$ is an operator that picks out the large $\bar n\cdot p$ label momentum of the fields it acts on [16], and $ig\mathcal{B}^{\perp\mu}_{n,\omega} = [1/\bar{\mathcal{P}}W_n^\dagger[i\bar n\cdot D_{c,n}, iD^\mu_{n,\perp}]W_n\delta(\omega - \bar{\mathcal{P}}^\dagger)]$. The b_v is an HQET b-quark field.

The leading order factorization theorem from SCET$_{\rm I}$ is [5]

$$A^{(0)} = \frac{G_F m_B^2 f_{M_1}}{\sqrt{2}}\Big[\int_0^1 du dz T_{1J}(u,z)\zeta^{BM_2}_J(z)\phi^{M_1}(u) + \int_0^1 du T_{1\zeta}(u)\zeta^{BM_2}\phi^{M_1}(u)\Big] + \{M_1 \leftrightarrow M_2\}. \quad (7)$$

Here T_{1J} and $T_{1\zeta}$ contain contributions from the hard scales m_b, and ϕ^M is the nonperturbative twist-2 light-cone distribution function. The terms ζ^{BM} and $\zeta^{BM}_J(z)$ contain contributions from both the intermediate scale $\mu_i \sim \sqrt{m_b\Lambda}$ and the scale Λ, and are defined by SCET$_{\rm I}$ matrix elements between B and M states. In particular,

[2] $\hat A_{c\bar c}$ has the c fields in $O^c_{1,2}$ and O_{3-10} replaced by nonrelativistic fields [5], and is suppressed by at least their relative velocity, $v \sim 0.3$–0.5. The possibility of large nonperturbative charm loop contributions was first discussed in Refs. [12,13], and the size of these terms remains controversial [25,26].

[3] Recall that, to derive the η^6, we note that $\lambda^8 = \eta^4$, and changing the scaling $\lambda \to \eta$ for four collinear quark fields in matching SCET$_{\rm I} \to$ SCET$_{\rm II}$ gives the extra η^2. The λ^7 term gains an extra λ from the change in scaling to a collinear $D_\perp$.

TABLE I. All contributions to $B \to M_1 M_2$ amplitudes at leading order ($A^{(0)}$) and at order Λ/m_b ($A^{(1)}$), besides $A_{c\bar{c}}$. In the first $A^{(1)}$ row, $j' + j + \sum k_i \leq 4$. The second column lists all $\mathrm{SCET_I}$ time-ordered products that can contribute to the amplitude at zeroth and first order in the power counting, as well as the local chirally enhanced operator that contributes at order Λ^2/m_b^2. The perturbative expansions of these contributions start with factors of α_s listed in the columns labeled "Peturbative order." In these columns, a factor of $1/\pi$ indicates a perturbative loop and "–" means that the time-ordered products first contribute at order α_s^3 or not at all. The "Dependence in $\mathrm{SCET_{II}}$" column lists the known dependence on nonperturbative parameters, with ... referring to nonperturbative inputs that have not yet been classified. The "Properties" column indicates whether at least one of the nonperturbative parameters is complex.

Order in Λ/m_b	Time-ordered products in $\mathrm{SCET_I}$	Perturbative order		Dependence in $\mathrm{SCET_{II}}$	Properties
		Annihilation	Other		
$A^{(0)}$	$Q_i^{(0)}\mathcal{L}_{\xi q}^{(1)}$, $Q_i^{(0)}\mathcal{L}_{\xi q}^{(2)}$, $Q_i^{(0)}\mathcal{L}_{\xi q}^{(1)}\mathcal{L}^{(1)}$	–	$\alpha_s(\mu_i)$	$\phi_i^B \phi_j^M \phi^{M'}$	Real
	$Q_i^{(1)}\mathcal{L}_{\xi q}^{(1)}$	–	$\alpha_s(\mu_i)$	$\phi_+^B \phi^M \phi^{M'}$	Real
$A^{(1)}$	$Q_i^{(j'=0,1)}\mathcal{L}_{\xi q}^{(j\leq 4)}\Pi_i \mathcal{L}^{(k_i)}$	–	$\alpha_s(\mu_i)$	...	Complex
	$Q_i^{(4)}$	$\alpha_s(\mu_h)$	–	$f_B \phi^M \phi^{M'}$	Real
	$Q_i^{(2)}\mathcal{L}_{\xi q}^{(1)}$	$\alpha_s(\mu_h)$	$\alpha_s(\mu_i)$	$\phi^B \phi^{3M} \phi^{M'}$	Real
	$Q_i^{(0)}[\mathcal{L}_{\xi q}^{(1)}]^3$, $Q_i^{(0)}[\mathcal{L}_{\xi q}^{(1)}]^3\mathcal{L}^{(1)}$	$\alpha_s^2(\mu_i)/\pi$	$\alpha_s^2(\mu_i)/\pi$	$S_j(k_{1,2}^+, k_3^-), \ldots$	Complex
	$Q_i^{(0)}[\mathcal{L}_{\xi q}^{(1)}]^2\mathcal{L}_{\xi q}^{(2)}$, $Q_i^{(1)}[\mathcal{L}_{\xi q}^{(1)}]^3$	$\alpha_s^2(\mu_i)/\pi$	$\alpha_s^2(\mu_i)/\pi$	$S_j(k_{1,2}^+, k_3^-), \ldots$	Complex
	$Q_i^{(2)}[\mathcal{L}_{\xi q}^{(1)}]^2$	–	$\alpha_s^2(\mu_i)/\pi$	...	Complex
	$Q_i^{(2)}\mathcal{L}_{\xi q}^{(1)}\mathcal{L}^{(1)}$, $Q_i^{(2)}\mathcal{L}_{\xi q}^{(2)}$, $Q_i^{(3)}\mathcal{L}_{\xi q}^{(1)}$	$\alpha_s(\mu_h)\alpha_s(\mu_i)/\pi$	$\alpha_s(\mu_i)$	...	Complex
$A^{(2)}$	$Q_i^{(5)}$	$\alpha_s(\mu_h)$	–	$f_B \mu_M \phi_{pp}^M \phi^{M'}$	Real

their scaling is

$$\zeta^{BM}(E), \zeta_J^{BM}(z, E) \sim \left(\frac{\Lambda}{m_b}\right)^{3/2}[\alpha_s(\mu_i) + \ldots], \qquad (8)$$

explaining the $\alpha_s(\mu_i)$ entry in the $A^{(0)}$ rows of Table I. The ζ^{BM} functions occur in both semileptonic decays and nonleptonic decays ($E \approx m_B/2$). Integrating out the scale $\sqrt{m_b \Lambda}$ to all orders in α_s by matching onto $\mathrm{SCET_{II}}$ gives [5,18]

$$\begin{aligned}\zeta_J^{BM}(z, E) &= \frac{f_B f_M m_B}{4E^2} \\ &\quad \times \int dx \int dk^+ J(z, x, k_+, E)\phi^M(x)\phi_+^B(k^+), \\ \zeta^{BM}(E) &= \frac{f_B f_M m_B}{4E^2}\sum_{a,b}\int dx_1 dx_2 \int dk_1^+ dk_2^+ J_{ab}(x_i, k_j^+, E) \\ &\quad \times \phi_a^M(x_i)\phi_b^B(k_j^+), \end{aligned} \qquad (9)$$

where the ϕ_a^M and ϕ_b^B's are twist-2 and twist-3, two- and three-parton distributions, and we pulled out $f_B f_M$ for convenience. The jet functions J, J_{ab} occur due to the time-ordered product structure in $\mathrm{SCET_I}$ and contain contributions from the scale $\sqrt{m_b \Lambda}$. Using the result for ζ_J^{BM} at order $\alpha_s(\mu_i)$ this result agrees with Ref. [2] (where expressing ζ^{BM} in terms of the full theory form factor generates an additional ζ_J^{BM} term). The result for ζ^{BM} in Eq. (9) was derived in Ref. [18] and required the MS factorization with zero-bin subtractions. The set of contributing functions (indices a, b) is determined by the complete set of $\mathrm{SCET_{II}}$ operators derived in Ref. [28]. The power counting in $\alpha_s(\mu_i)$ for the $\mathrm{SCET_I}$ functions ζ^{BM} and ζ_J^{BM} agrees with that derived in pQCD [29].

Next we classify the contributions to the power suppressed $B \to M_1 M_2$ amplitudes $A^{(1)}$. In $\mathrm{SCET_I}$ we need to study operators and time-ordered products with scaling up to $\mathcal{O}(\lambda^{10})$. These have one or three light usoft quark fields. The relevant terms are listed in Table I, where $Q_i^{(j)} \sim \lambda^{6+j}$ and our notation for the Lagrangians up to second order is taken from Ref. [30]. All the listed terms have an odd number of soft light quark fields. A basis for the $Q_i^{(4)}$ operators is constructed in Sec. III, for the $Q_i^{(2)}\mathcal{L}_{\xi q}^{(1)}$ terms in Ref. [19], and for the $Q_i^{(5)}$ terms in Sec. IV. A basis is not yet known for the remaining $Q_i^{(2)}$ operators, for $Q_i^{(3)}$, and for the $\mathcal{L}_{\xi q}^{(3,4)}$ and $\mathcal{L}^{(3)}$ Lagrangians, but they do not contribute at $\mathcal{O}(\alpha_s)$, and only general properties of these operators are required for our analysis. Dashes in Table I indicate terms that are absent to all orders in α_s for reasons to be explained below. To determine the perturbative order listed in the table, we count the number of hard $\alpha_s(\mu_h)$ factors from the matching onto $\mathrm{SCET_I}$, and the number of intermediate scale $\alpha_s(\mu_i)$ factors from matching onto $\mathrm{SCET_{II}}$. The "Dependence in $\mathrm{SCET_{II}}$" column lists the nonperturbative quantities that appear in the factorization theorem for the leading order result described above, and from the factorization theorems we will derive in Secs. III and IV below. The "Properties" column lists whether the nonperturbative distribution functions are complex or real as described in detail in Sec. V, and has implications for strong phase information in the power corrections. The results in Table I imply the following power counting

(for amplitudes not involving $A_{c\bar{c}}$),

$$\mathrm{Re}[\hat{A}^{(0)}] \sim \alpha_s(\mu_i), \quad \mathrm{Im}[\hat{A}^{(0)}] \sim \alpha_s(\mu_i)\alpha_s(\mu_h),$$
$$\mathrm{Re}[\hat{A}^{(1)}_{\mathrm{ann}}] \sim [\alpha_s(\mu_h) + \alpha_s^2(\mu_i)]\frac{\Lambda}{m_b}, \quad \mathrm{Im}[\hat{A}^{(1)}_{\mathrm{ann}}] \sim \alpha_s^2(\mu_i)\frac{\Lambda}{m_b},$$
$$\mathrm{Re}[\hat{A}^{(1)}_{\mathrm{rest}}] \sim \alpha_s(\mu_i)\frac{\Lambda}{m_b}, \quad \mathrm{Im}[\hat{A}^{(1)}_{\mathrm{rest}}] \sim \alpha_s(\mu_i)\frac{\Lambda}{m_b}. \tag{10}$$

To facilitate the discussion we divide the annihilation amplitudes into local annihilation contributions, $A^{(1,2)}_{\mathrm{Lann}}$ from the operators $Q_i^{(4,5)}$ that are insensitive to the jet scale, and into the remaining annihilation amplitudes, $A^{(1)}_{\mathrm{Tann}}$, which are from time-ordered products in $\mathrm{SCET_I}$. Thus,

$$A^{(1)}_{\mathrm{ann}} = A^{(1)}_{\mathrm{Lann}} + A^{(1)}_{\mathrm{Tann}}. \tag{11}$$

In the literature [7,8,10,11,31] only local annihilation amplitudes have been studied, and their matrix elements were parametrized by complex amplitudes. In SCET, $Q_i^{(4)}$ is a six-quark operator with one usoft quark, such as

$$(\bar{d}_s \Gamma_s b_v)(\bar{u}_{\bar{n},\omega_2}\Gamma_{\bar{n}} q_{\bar{n},\omega_3})(\bar{q}_{n,\omega_1}\Gamma_n u_{n,\omega_4}), \tag{12}$$

where other $Q_i^{(4)}$ operators have different flavor structures. To derive the power counting for this operator, start with $Q^{(0)} \sim \lambda^6$, then note that switching a collinear quark to a usoft quark costs λ^2, and adding a ξ_n and $\xi_{\bar{n}}$ from a hard gluon also costs λ^2. This yields $Q_i^{(4)} \sim \mathcal{O}(\alpha_s(\mu_h)\lambda^{10})$. In matching onto $\mathrm{SCET_{II}}$ we simply replace $Q_i^{(4)} \to O_i^{(1L)} \sim \eta^7$, with the operator having an identical form. $\mathrm{SCET_I}$ operators $Q_i^{(4)}$ that do not have the form in Eq. (12) exist, but they must be taken in time-ordered products with a subleading Lagrangian and so do not contribute to $A^{(1)}$. For this reason all local operator contributions to $A^{(1)}$ contribute in the annihilation terms and not in $A^{(1)}_{\mathrm{rest}}$. Since the matching onto $O_i^{(1L)}$ is local, it appears as in Fig. 1(a) with an $\alpha_s(\mu_h)$, but with no jet function. Thus this contribution to $A^{(1)}_{\mathrm{ann}}$ is of order $\alpha_s(\mu_h)/\alpha_s(\mu_i)\Lambda/m_b$ relative to $A^{(0)}$. In Sec. III we construct a complete basis of $Q_i^{(4)}$ operators and show that their matrix elements are factorizable in SCET at any order in perturbation theory, and do not generate strong phases at $\mathcal{O}(\alpha_s(\mu_h))$. We prove a similar theorem for chirally enhanced terms in the set $Q_i^{(5)}$ in Sec. IV.

The annihilation amplitudes and other Λ/m_b suppressed amplitudes also occur through time-ordered products. Two examples are shown by Figs. 1(b) and 1(c). A subset of these terms were considered in Ref. [15], including the diagram in Fig. 1(c), and the phenomenological impact of these power corrections was studied. So far, no attempt has been made to work out the strong phase properties and perturbative orders in α_s of the time-ordered products, a task we take up here. A complete classification of time-ordered products for the leading power corrections to $B \to M_1 M_2$ is listed in Table I. A subset of these terms contribute to the annihilation amplitudes. To see which, we note that terms with a $Q_i^{(0,1)}$ and only one $\mathcal{L}^{(1)}_{\xi q}$ do not contribute to annihilation at either leading or next-to-leading order; the weak operator is not high enough order in λ to contain an extra $n - \bar{n}$ pair, and there are not enough $\mathcal{L}_{\xi q}$'s to produce the pair through a soft quark exchange. To rule out these terms it is important that we are not considering

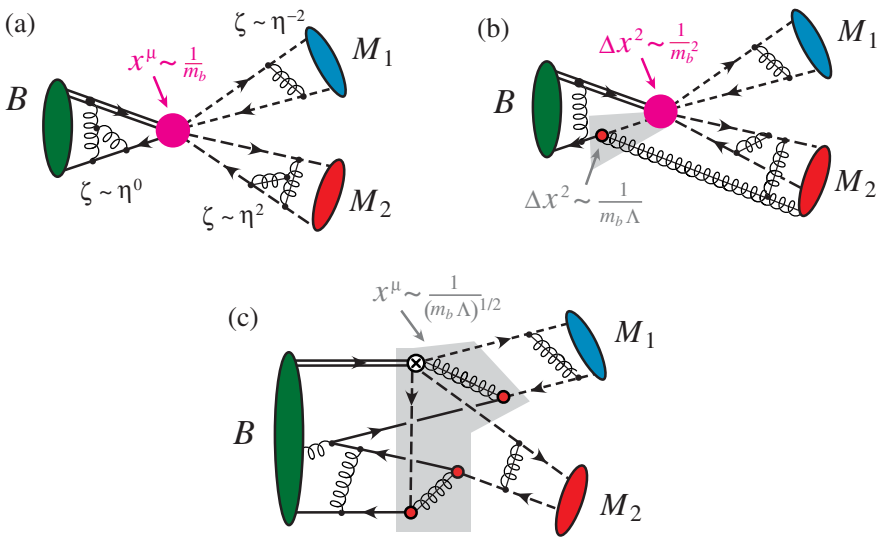

FIG. 1 (color online). Three types of factorization contributions to annihilation amplitudes which are the same order in $\eta = \Lambda_{\mathrm{QCD}}/m_b$. (a) shows $Q_i^{(4)}$ which has ≥ 1 hard gluon and factorizes at the scale m_b. The rapidity parameter, $\zeta = p^-/p^+$, controls the MS factorization between soft momenta (B), n-collinear momenta (M_2), and $\bar{n}$-collinear momenta (M_1). (b) shows the time-ordered product $Q_i^{(2)}\mathcal{L}^{(1)}_{\xi q}$, which involves factorization at m_b and $\sqrt{m_b\Lambda}$. (c) shows the time-ordered product $Q_i^{(1)}[\mathcal{L}^{(1)}_{\xi q}]^3$, which factorizes at the scale $\sqrt{m_b\Lambda}$ and does not need a hard gluon. Graphs (a) and (b) are of order $\alpha_s(\mu_h)$, while (c) is $\alpha_s(\mu_i)^2$.

isosinglet final states, which receive emission-annihilation contributions already at leading order. The term $Q_i^{(2)}[\mathcal{L}_{\xi q}^{(1)}]^2$ does not contribute to annihilation because we find that all annihilation-type contractions are further power suppressed when matched onto $\mathrm{SCET_{II}}$.

Time-ordered products with either a $Q^{(j\geq 2)}$ or with three $\mathcal{L}_{\xi q}$'s do contribute to annihilation. Examples of these two types are shown in Figs. 1(b) and 1(c). Compared to the local annihilation amplitude from $Q_i^{(4)}$, only the time-ordered product $Q^{(2)}\mathcal{L}_{\xi q}^{(1)}$ contributes at the same order in α_s. To demonstrate this, note that for terms with three $\mathcal{L}_{\xi q}$'s all graphs have at least two contracted hard-collinear gluons and so are $\mathcal{O}(\alpha_s^2(\mu_i))$. Graphs with a $Q^{(2,3)}$ start with one $\alpha_s(\mu_h)$, and will also have an additional $\alpha_s(\mu_i)$ from a hard-collinear gluon, unless it remains uncontracted in matching onto $\mathrm{SCET_{II}}$. The uncontracted gluon costs an additional λ in the matching onto $\mathrm{SCET_{II}}$, so only the time-ordered product $Q^{(2)}\mathcal{L}_{\xi q}^{(1)}$ can have a leading, $\mathcal{O}(\alpha_s(m_b))$, contribution. Figure 1(b) gives an example of a diagram occurring from this time-ordered product. The resulting amplitude involves the three-parton distribution, ϕ_{3M_2}. As shown in Ref. [19] it also involves the twist-2 distribution ϕ_B^+, and its leading order convolution integrals converge.

The time-ordered products with three $\mathcal{L}_{\xi q}$'s are suppressed by $\alpha_s^2(\mu_i)/\alpha_s(\mu_h)$ relative to $Q_i^{(4)}$, and can be proven to involve a complex nonperturbative function, as labeled in Table I [an example is shown in Fig. 1(c)]. Thus, if perturbation theory converges rapidly at the scale μ_i, then complex annihilation amplitudes are highly suppressed. If perturbation theory at μ_i is poorly convergent, then the time-ordered product contribution could be important numerically, comparable or even larger than the leading local annihilation amplitude from $Q_i^{(4)}$. Local annihilation contributions are discussed in detail in Secs. III and IV, while strong phase properties of the amplitudes and the time-ordered product contributions are taken up in Sec. V.

III. LOCAL SIX-QUARK OPERATORS IN $\mathrm{SCET_{II}}$

In this section we construct a complete basis of $O_i^{(1L)}$ operators in $\mathrm{SCET_{II}}$ (the $Q_i^{(4)}$ terms in $\mathrm{SCET_I}$) and derive a factorization theorem for their contributions to $B\to M_1M_2$. To find a complete basis we consider color, spin, and flavor structures that could appear when matching at any order in α_s. Color is simple; the six-quark operator must have $\Gamma_s\otimes\Gamma_{\bar n}\otimes\Gamma_n = 1\otimes 1\otimes 1$. Although operators with a T^A in one or more bilinears are allowed at this order, with the factorization properties of the leading Lagrangians and $\langle M_nM_{\bar n}|O|B_s\rangle = \langle 0|\ldots|B_s\rangle\langle M_{\bar n}|\ldots|0\rangle\langle M_n|\ldots|0\rangle$, the terms with T^A's give a vanishing matrix element between the color singlet hadronic states [1].

For spin we start by looking at chirality which is preserved by the matching at m_b. Since there is no jet function, the soft field that interpolates for the spectator quark in the B meson must come from the original operator in H_W. Fierz identities allow us to choose a basis in which this spectator field is always in a bilinear with the b-quark field. To be definite, we take the other $\bar\psi$ field from H_W to go in the $\bar n$ direction (in the SCET Hamiltonian we sum over $n\leftrightarrow\bar n$). This implies that the pair-produced quark is in the n direction. For $O_{1-4,9,10}$ the allowed chiral structures induced in SCET by matching are $(LH)(LL)(LL)$ and $(LH)(LR)(RL)$ where L and R correspond to the handedness for the light quarks in the bilinears in the order shown in Eq. (12). We cannot assign a handedness to the heavy quark denoted here by H. For O_{5-8} we can have $(LH)\times(RL)(LR)$, $(LH)(RR)(RR)$, $(RH)(LL)(LR)$, and $(RH)\times(LR)(RR)$. A complete basis of Dirac structures for the individual bilinears is

$$\Gamma_s = \gamma^\alpha, \qquad \Gamma_{\bar n} = \{\not{\bar n}, \not{\bar n}\gamma_\perp^\nu\}, \qquad \Gamma_n = \{\not n, \not n\gamma_\perp^\mu\}. \quad (13)$$

Structures with γ_5 are not needed because we have specified the handedness. Here $\not n\gamma_\perp^\mu$ and $\not{\bar n}\gamma_\perp^\nu$ connect left- and right-handed quarks, while $\not n$ and $\not{\bar n}$ connect quarks of the same handedness. From the basis in Eq. (13) we must construct an overall scalar using the tensors v^μ, n^μ, $\bar n^\mu$, $g_\perp^{\mu\nu}$, and $\epsilon_\perp^{\mu\nu}\equiv\epsilon^{\mu\nu\alpha\beta}\bar n_\alpha n_\beta/2$. We take $\epsilon^{0123}=1$, and work in a frame where $v_\perp^\mu = 0$ and $n\cdot v = \bar n\cdot v = 1$, which makes the set $\{n, \bar n, v\}$ redundant. For reasons that will become apparent, we pick v^μ and $(n^\mu - \bar n^\mu)$ as our basis in this section. The definite handedness allows us to turn any contraction involving $i\epsilon_\perp^{\mu\nu}$ into a contraction with $g_\perp^{\mu\nu}$, for example, $i\epsilon_\perp^{\mu\nu}\bar\xi_n^L\not{\bar n}\gamma_\nu^\perp\xi_n^R = \bar\xi_n^L\not{\bar n}\gamma_\perp^\mu\gamma_5\xi_n^R = \bar\xi_n^L\not{\bar n}\gamma_\perp^\mu\xi_n^R$. The $(LH)(LR)(RL)$ and $(LH)(RL)(LR)$ structures can be ruled out since

$$\not{\bar n}\gamma_\perp^\mu P_R\otimes\not{\bar n}\gamma_\mu^\perp P_L = \not{\bar n}\gamma_\perp^\mu P_L\otimes\not{\bar n}\gamma_\mu^\perp P_R = 0. \quad (14)$$

Noting that $\not v h_v = h_v$ this leaves four allowed spin structures,

$$\Gamma_s\otimes\Gamma_{\bar n}\otimes\Gamma_n = \{1\otimes\not{\bar n}\otimes\not n, (\not n - \not{\bar n})\otimes\not{\bar n}\otimes\not n, \gamma_\perp^\alpha\otimes\not{\bar n}\otimes\not n\gamma_\alpha^\perp, \gamma_\perp^\alpha\otimes\not{\bar n}\gamma_\alpha^\perp\otimes\not n\}. \quad (15)$$

The last two structures have $\bar q_s\gamma_\perp^\alpha b_v$ and vanish identically for B-meson decays (they would contribute for B^*'s). Furthermore, the local annihilation operators are not sensitive to the k^+ momentum of the soft spectator quark. Thus in taking the matrix element we can use

$$\langle 0|\bar q_s\gamma_5 h_v|B\rangle = -im_Bf_B, \qquad \langle 0|\bar q_s\gamma_5(\not n - \not{\bar n})h_v|B\rangle = 0. \quad (16)$$

Here f_B is the decay constant in the heavy quark limit. The fact that we can match onto a basis of local SCET operators of the form in Eq. (12) demonstrates to all orders in α_s that the local annihilation contributions are proportional to f_B. Using Eq. (16) the second Dirac structure in Eq. (15) is

eliminated, so we do not list operators with $(\not{n} - \not{\bar{n}})$ in the soft bilinears below.

Next we consider the allowed flavor structures. From the operators $O_{1,2}$ we have $(\bar{u}b)(\bar{d}q)(\bar{q}u)$, $(\bar{d}b)(\bar{u}q)(\bar{q}u)$, from $O_{1-6,7\gamma,8g}$ we have $(\bar{d}b)(\bar{q}'q)(\bar{q}q')$, $(\bar{q}'b)(\bar{d}q)(\bar{q}q')$, and O_{7-10} give a combination of these. Here $q'\bar{q}'$ appeared in the weak operator, while $q\bar{q}$ is the pair produced in the matching onto SCET. Thus a basis for B-decay operators is

$$
\begin{aligned}
O_{1d}^{(1L)} &= \frac{2}{m_b^3}\sum_q [\bar{d}_s P_R b_v][\bar{u}_{\bar{n},\omega_2}\not{n} P_L q_{\bar{n},\omega_3}][\bar{q}_{n,\omega_1}\not{\bar{n}} P_L u_{n,\omega_4}],\\
O_{2d}^{(1L)} &= \frac{2}{m_b^3}\sum_q [\bar{u}_s P_R b_v][\bar{d}_{\bar{n},\omega_2}\not{n} P_L q_{\bar{n},\omega_3}][\bar{q}_{n,\omega_1}\not{\bar{n}} P_L u_{n,\omega_4}],\\
O_{3d}^{(1L)} &= \frac{2}{m_b^3}\sum_{q,q'} [\bar{d}_s P_R b_v][\bar{q}'_{\bar{n},\omega_2}\not{n} P_L q_{\bar{n},\omega_3}][\bar{q}_{n,\omega_1}\not{\bar{n}} P_L q'_{n,\omega_4}],\\
O_{4d}^{(1L)} &= \frac{2}{m_b^3}\sum_{q,q'} [\bar{q}'_s P_R b_v][\bar{d}_{\bar{n},\omega_2}\not{n} P_L q_{\bar{n},\omega_3}][\bar{q}_{n,\omega_1}\not{\bar{n}} P_L q'_{n,\omega_4}],\\
O_{5d}^{(1L)} &= \frac{2}{m_b^3}\sum_q [\bar{d}_s P_R b_v][\bar{u}_{\bar{n},\omega_2}\not{n} P_R q_{\bar{n},\omega_3}][\bar{q}_{n,\omega_1}\not{\bar{n}} P_R u_{n,\omega_4}],\\
O_{6d}^{(1L)} &= \frac{2}{m_b^3}\sum_q [\bar{u}_s P_R b_v][\bar{d}_{\bar{n},\omega_2}\not{n} P_R q_{\bar{n},\omega_3}][\bar{q}_{n,\omega_1}\not{\bar{n}} P_R u_{n,\omega_4}],\\
O_{7d}^{(1L)} &= \frac{2}{m_b^3}\sum_{q,q'} [\bar{d}_s P_R b_v][\bar{q}'_{\bar{n},\omega_2}\not{n} P_R q_{\bar{n},\omega_3}][\bar{q}_{n,\omega_1}\not{\bar{n}} P_R q'_{n,\omega_4}],\\
O_{8d}^{(1L)} &= \frac{2}{m_b^3}\sum_{q,q'} [\bar{q}'_s P_R b_v][\bar{d}_{\bar{n},\omega_2}\not{n} P_R q_{\bar{n},\omega_3}][\bar{q}_{n,\omega_1}\not{\bar{n}} P_R q'_{n,\omega_4}].
\end{aligned}
\tag{17}
$$

Here we integrated out c and b quarks in the sum over flavors, so the remaining sums are over $q = u, d, s$ and $q' = u, d, s$. For the $\Delta S = 0$ effective Hamiltonian with Wilson coefficients $a_i^{(d)}(\omega_j)$ we use the notation

$$
H_W = \frac{4G_F}{\sqrt{2}}\sum_{n,\bar{n}}\int [d\omega_1 d\omega_2 d\omega_3 d\omega_4]\sum_{i=1-8} a_i^d(\omega_j) O_{id}^{(1L)}(\omega_j).
\tag{18}
$$

To pull the Cabibbo-Kobayashi-Maskawa (CKM) structures out of the SCET Wilson coefficients we write

$$
a_i^d(\omega_j) = \begin{cases} \lambda_u^{(d)} a_{iu}(\omega_j) + \lambda_c^{(d)} a_{ic}(\omega_j) & [i = 1, 2, 3, 4], \\ (\lambda_u^{(d)} + \lambda_c^{(d)}) a_i(\omega_j) & [i = 5, 6, 7, 8], \end{cases}
\tag{19}
$$

where $\lambda_p^{(d)} = V_{pb}V_{pd}^*$. Identical definitions for a_i^s are made by replacing $\lambda_u^{(d)} \to \lambda_u^{(s)}$ and $\lambda_c^{(d)} \to \lambda_c^{(s)}$. For $i = 5, 6, 7, 8$ only penguin operators contribute.

Next we take the $B \to M_1 M_2$ matrix element of H_W. The factorization properties of SCET yield

$$
\begin{aligned}
\langle M_1 M_2 | O_{1d}^{(1L)} | B\rangle = \frac{2}{m_b^3}\sum_q & \langle M_1 | \bar{u}_{\bar{n},\omega_2}\not{n} P_L q_{\bar{n},\omega_3} | 0\rangle \\
& \times \langle M_2 | \bar{q}_{n,\omega_1}\not{\bar{n}} P_L u_{n,\omega_4} | 0\rangle \\
& \times \langle 0 | \bar{d}_s P_R b_v | B\rangle + \{M_1 \leftrightarrow M_2\},
\end{aligned}
\tag{20}
$$

with similar results for the other $O_{id}^{(1L)}$ terms. Here the $\{M_1 \leftrightarrow M_2\}$ indicates terms where the flavor quantum numbers of the M_2 state match those of the $\bar{n}$-collinear operator. The matrix elements in Eq. (20) are zero for transversely polarized vector mesons in agreement with the helicity counting in Ref. [31]. Equation (20) can be evaluated using Eq. (16) and

$$
\begin{aligned}
\langle P_{n_1}(p) | \bar{q}_{n,\omega}^{(f)}\not{\bar{n}} P_{L,R} q_{n,\omega'}^{(f')} | 0\rangle &= \frac{\pm i f_P}{2} c_{Pff'}\delta_{nn_1} \\
&\quad \times \delta(\bar{n}\cdot p - \omega + \omega')\phi_P(y), \\
\langle V_{n_1}(p,\varepsilon) | \bar{q}_{n,\omega}^{(f)}\not{\bar{n}} P_{L,R} q_{n,\omega'}^{(f')} | 0\rangle &= \frac{i f_V m_V \bar{n}\cdot\varepsilon}{2\bar{n}\cdot p} c_{Vff'}\delta_{nn_1} \\
&\quad \times \delta(\bar{n}\cdot p - \omega + \omega')\phi_{V_\parallel}(y).
\end{aligned}
\tag{21}
$$

Here f, f' are flavor indices, $\phi_P(y)$ and $\phi_{V_\parallel}(y)$ are the twist-2 light-cone distribution functions for pseudoscalars and vectors, $y = \omega/\bar{n}\cdot p = \omega/m_b$, and $c_{Pff'}$, $c_{Vff'}$ are Clebsch-Gordan coefficients. For the M_2 mesons, P_{n_2} and V_{n_2}, we have the same equation with $n \leftrightarrow \bar{n}$, and $y \to x$. Since the $P_{L,R}$ only induce $\pm$ signs in the pseudoscalar matrix element, it is convenient to define

$$
\begin{aligned}
\tilde{a}_1^{\,d} &= a_1^d + \kappa a_5^d, & \tilde{a}_2^d &= a_2^d + \kappa a_6^d, \\
\tilde{a}_3^d &= a_3^d + \kappa a_7^d, & \tilde{a}_4^d &= a_4^d + \kappa a_8^d,
\end{aligned}
\tag{22}
$$

with similar definitions for $\tilde{a}_i^s$. Here $\kappa = +1$ for PP, VV, and $\kappa = -1$ for PV channels. Using these results, the $\mathcal{O}(\Lambda/m_b)$ local annihilation amplitudes are

$$
\begin{aligned}
A_{\mathrm{Lann}}^{(1)}(\bar{B} \to M_1 M_2) = & -\frac{G_F f_B f_{M_1} f_{M_2}}{\sqrt{2}} \\
& \times \int_0^1 dx dy H(x,y)\phi^{M_1}(y)\phi^{M_2}(x).
\end{aligned}
\tag{23}
$$

Here $H(x, y)$ are perturbatively calculable hard coefficients determined by the SCET Wilson coefficients $\tilde{a}_i(\omega_j)$. Results for different final states are listed in Table II for $\bar{B}^0$ and B^- decays, and in Table III for $\bar{B}_s$ decays. Our derivation of the local annihilation amplitude in Eq. (23) is valid to all orders in α_s, and provides a proof of factorization for this term.

Matching at tree level involves computing the $\mathcal{O}(\alpha_s(m_b))$ graphs in Fig. 2 and comparing them with matrix elements of the SCET operators $Q_i^{(4)}$. Doing so, we find that the Wilson coefficients $a_i(x, y)$ are

TABLE II. Hard functions for $\bar{B}^0$ and B^- decays for the annihilation amplitude $A^{(1)}_{\rm Lann}$ in Eq. (23). For each pair of mesons in the table, the first is M_1 and the second M_2.

$M_1 M_2$	$H(x,y)$
$\pi^-\pi^+$, $\pi^-\rho^+$, $\rho^-\pi^+$, $\rho^-\rho^+$	$-\tilde{a}_1^d(x,y) - \tilde{a}_4^d(y,x) - \tilde{a}_3^d(x,y) - \tilde{a}_3^d(y,x)$
$\pi^-\pi^0$, $\rho^-\pi^0$, $\pi^-\rho^0$, $\rho_\parallel^-\rho_\parallel^0$	$\frac{1}{\sqrt{2}}[\tilde{a}_2^d(x,y) + \tilde{a}_4^d(x,y) - \tilde{a}_2^d(y,x) - \tilde{a}_4^d(y,x)]$
$\pi^0\pi^0$, $\pi^0\rho^0$, $\rho^0\rho^0$	$[\frac{1}{2}\tilde{a}_1^d(x,y) + \tilde{a}_3^d(x,y) + \frac{1}{2}\tilde{a}_4^d(x,y)] + [x \leftrightarrow y]$
$K^{(*)-}K^{(*)+}$	$-\tilde{a}_1^d(x,y) - \tilde{a}_3^d(x,y) - \tilde{a}_3^d(y,x)$
$\bar{K}^{(*)0}K^{(*)0}$	$\tilde{a}_3^d(x,y) + \tilde{a}_3^d(y,x) + \tilde{a}_4^d(x,y)$
$K^{(*)-}K^{(*)0}$	$\tilde{a}_2^d(x,y) + \tilde{a}_4^d(x,y)$
$\pi^-\bar{K}^{(*)0}$, $\rho^-\bar{K}^{(*)0}$	$\tilde{a}_2^s(x,y) + \tilde{a}_4^s(x,y)$
$\pi^0\bar{K}^{(*)-}$, $\rho^0 K^{(*)-}$	$-\frac{1}{\sqrt{2}}[\tilde{a}_2^s(x,y) + \tilde{a}_4^s(x,y)]$
$\pi^0\bar{K}^{(*)0}$, $\rho^0\bar{K}^{(*)0}$	$\frac{1}{\sqrt{2}}\tilde{a}_4^s(x,y)$
$\pi^+K^{(*)-}$, $\rho^+K^{(*)-}$	$-\tilde{a}_4^s(x,y)$

TABLE III. Hard functions for $\bar{B}_s$ decays for the annihilation amplitude $A^{(1)}_{\rm Lann}$ in Eq. (23).

$M_1 M_2$	$H(x,y)$
$\pi^-K^{(*)+}$, $\rho^-K^{(*)+}$	$-\tilde{a}_4^d(y,x)$
$\pi^0K^{(*)0}$, $\rho^0K^{(*)0}$	$\frac{1}{\sqrt{2}}\tilde{a}_4^d(y,x)$
$\pi^-\pi^+$, $\pi^-\rho^+$, $\rho^-\pi^+$, $\rho^-\rho^+$	$-\tilde{a}_1^s(x,y) - \tilde{a}_3^s(x,y) - \tilde{a}_3^s(y,x)$
$\pi^0\pi^0$, $\pi^0\rho^0$, $\rho^0\rho^0$	$[\frac{1}{2}\tilde{a}_1^s(x,y) + \tilde{a}_3^s(x,y)] + [x \leftrightarrow y]$
$K^{(*)-}K^{(*)+}$	$-\tilde{a}_1^s(x,y) - \tilde{a}_4^s(y,x) - \tilde{a}_3^s(x,y) - \tilde{a}_3^s(y,x)$
$\bar{K}^{(*)0}K^{(*)0}$	$\tilde{a}_3^s(x,y) + \tilde{a}_3^s(y,x) + \tilde{a}_4^s(y,x)$

$$
\begin{aligned}
a_{1u} &= \frac{C_F\pi\alpha_s(\mu_h)}{N_c^2}F(x,y)\Big(C_1+\frac{3}{2}C_{10}\Big), \qquad a_{1c} = \frac{C_F\pi\alpha_s(\mu_h)}{N_c^2}F(x,y)\Big(\frac{3}{2}C_{10}\Big),\\
a_{2u} &= \frac{C_F\pi\alpha_s(\mu_h)}{N_c^2}F(x,y)\Big(C_2+\frac{3}{2}C_9\Big), \qquad a_{2c} = \frac{C_F\pi\alpha_s(\mu_h)}{N_c^2}F(x,y)\Big(\frac{3}{2}C_9\Big),\\
a_{3u} &= \frac{C_F\pi\alpha_s(\mu_h)}{N_c^2}F(x,y)\Big(C_4-\frac{1}{2}C_{10}\Big), \qquad a_{3c} = \frac{C_F\pi\alpha_s(\mu_h)}{N_c^2}F(x,y)\Big(C_4-\frac{1}{2}C_{10}\Big),\\
a_{4u} &= \frac{C_F\pi\alpha_s(\mu_h)}{N_c^2}F(x,y)\Big(C_3-\frac{1}{2}C_9\Big), \qquad a_{4c} = \frac{C_F\pi\alpha_s(\mu_h)}{N_c^2}F(x,y)\Big(C_3-\frac{1}{2}C_9\Big),\\
a_5 &= \frac{C_F\pi\alpha_s(\mu_h)}{N_c^2}F(\bar{y},\bar{x})\Big(\frac{3}{2}C_8\Big), \qquad a_6 = 0, \qquad a_7 = \frac{C_F\pi\alpha_s(\mu_h)}{N_c^2}F(\bar{y},\bar{x})\Big(C_6-\frac{1}{2}C_8\Big), \qquad a_8 = 0,
\end{aligned}
\tag{24}
$$

where $\mu_h \sim m_b$, $\bar{x} = 1-x$, $\bar{y} = 1-y$, with quark momentum fractions x and y as defined in Eq. (21) and shown in Fig. 2. The function F is

$$
F(x,y) = \left[\frac{1}{\bar{x}^2 y} - \frac{1}{y(x\bar{y}-1)}\right]_\text{ø} + \frac{d(\mu_-)\delta'(\bar{x})}{y}, \tag{25}
$$

where the ø notation and term involving the Wilson coefficient $d(\mu_-)$ are discussed below. The function $F(\bar{y},\bar{x})$ will involve $d(\mu_+)$. Note that the coefficients $a_{3u,3c,4u,4c,7,8}$ are polluted in the sense of Ref. [5], meaning that $\mathcal{O}(\alpha_s^2)$ matching results proportional to the large coefficients $C_{1,2}$ could compete numerically. The others are not polluted: $a_{1u,2u}$ involve $C_{1,2}$ at $\mathcal{O}(\alpha_s)$, while $a_{1c,2c,5,6}$ only get contributions from electroweak penguins. Our results for the diagrams in Fig. 2 agree with Refs. [7,10]. This includes the appearance of the combinations of momentum fractions in the functions $F(x,y)$ and $F(\bar{y},\bar{x})$, up to ø-distribution and d-term. For later convenience we define moment parameters which convolute the hard coefficients with the meson distributions

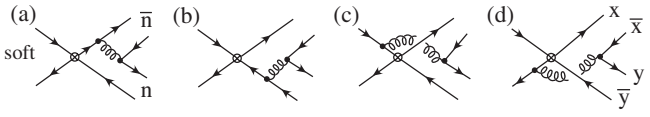

FIG. 2. Tree-level annihilation graphs for $B \to M_1 M_2$ decays. Here, soft, n, $\bar{n}$ denote quarks that are soft, n-collinear, and $\bar{n}$-collinear, respectively.

$$\beta_{iu}^{M_1M_2} = \int_0^1 dxdy[a_{iu}(x,y) + \kappa a_{i+4}(x,y)]\phi^{M_1}(y)\phi^{M_2}(x),$$
$$\beta_{ic}^{M_1M_2} = \int_0^1 dxdy[a_{ic}(x,y) + \kappa a_{i+4}(x,y)]\phi^{M_1}(y)\phi^{M_2}(x). \tag{26}$$

In Eq. (25) the subscript ø denotes the fact that singular terms in convolution integrals are finite in SCET due to the MS factorization which involves convolution integrals such as

$$\sum_{x,x'\neq 0}\int dx_r dx_r' \delta(1-x-x')\frac{\phi_M(x,x',\mu)}{\bar{x}^2}, \tag{27}$$

where $x^{(\prime)}$ and $x_r^{(\prime)}$ correspond to label and residual momenta [18]. Implementing $x \neq 0$ and $x' \neq 0$ in the MS-factorization scheme requires zero-bin subtractions, and divergences in the rapidity must also be regulated. The δ-function sets $x' = 1 - x$, so $x' \neq 0$ enforces $x \neq 1$. With the usual assumption that $\phi_M(x)$ vanishes at its endpoints with a powerlike falloff slower than quadratic, only integrals over $1/\bar{x}^2$ in $F(x,y)$ and $1/y^2$ in $F(\bar{y},\bar{x})$ require special care,

$$\langle \bar{x}^{-2}\rangle^M = \int_0^1 dx \frac{\phi_M(x,\mu)}{(\bar{x}^2)_\text{ø}},$$
$$\langle y^{-2}\rangle^M = \int_0^1 dy \frac{\phi_M(x,\mu)}{(y^2)_\text{ø}}. \tag{28}$$

The resulting moments $\langle \bar{x}^{-2}\rangle^M$ and $\langle y^{-2}\rangle^M$ should be considered hadronic parameters, for which we use the minimal subtraction scheme. Their value depends on μ and $\mu_\pm$ and are scheme dependent beyond the usual $\overline{\text{MS}}$ scheme for ϕ_M. This can be viewed as a modification of the distribution function, $\phi_M(x,\mu) \to \phi_M(x,\mu,\mu_-)$, where the x^{-2} moment of $\phi_M(x,\mu,\mu_-)$ converges. In order to derive a result that makes it easy to find a model for these moments, we follow Ref. [18] and assume there is no interference between the rapidity renormalization and invariant mass renormalization, which gives

$$\langle \bar{x}^{-2}\rangle^M = \int_0^1 dx \frac{\phi_M(x,\mu) + \bar{x}\phi_M'(1,\mu)}{\bar{x}^2} - \phi_M'(1,\mu)\ln\left(\frac{\bar{n}\cdot p_M}{\mu_-}\right),$$
$$\langle y^{-2}\rangle^M = \int_0^1 dy \frac{\phi_M(y,\mu) - y\phi_M'(0,\mu)}{y^2} + \phi_M'(0,\mu)\ln\left(\frac{n\cdot p_M}{\mu_+}\right). \tag{29}$$

Here $\phi_M'(1)$ is generated by a zero-bin subtraction which avoids double counting the region where $\bar{x} \to 0$. When $\bar{x} \to 0$ the corresponding outgoing quark becomes soft, and this contribution is taken into account by a time-ordered product term in Table I. To obtain the renormalized $\langle \bar{x}^{-2}\rangle^M$ result in Eq. (29) requires $1/\epsilon_\text{UV}$ counterterms which correspond to operators with the $\bar{n}$-collinear bilinears in Eq. (17), $[\bar{u}_{\bar{n},\omega_2}\not{n}\gamma_5 q_{\bar{n},\omega_3}]$ etc., which can be written as [18]

$$O_\text{ct} = \frac{\partial}{\partial\omega_3}(\bar{\xi}_{\bar{n}}W)_{\omega_2}\not{n}\gamma_5(W^\dagger\xi_{\bar{n}})_{\omega_3}\Big|_{\omega_3\to 0}. \tag{30}$$

The matrix element of these terms is taken prior to performing the partial derivative and the limit $\omega_3 \to 0$, and gives $\phi_M'(1,\mu)$. These terms do not have an $\omega_3 \neq 0$ restriction, and consistency of the renormalization procedure used to obtain Eq. (29) demands that the fields here are $\bar{n}$ collinear. An analogous set of terms are required for $\phi_M'(0,\mu)$. These terms are real at any scale, which follows from the requirements discussed in Sec. V for an SCET_II operator to be able to generate a physical strong phase. The dependences on $\mu_\pm$ in Eq. (29) are canceled by the leading dependences on these scales, $d(\mu_-) = \ln(p_M^-/\mu_-) + \kappa$ and $d(\mu_+) = \ln(p_M^+/\mu_+) + \kappa$, which appeared in Eq. (25). Here κ can be fixed by a matching computation. The $d(\mu_\pm)$ correspond to the renormalized coefficients of the O_ct, and must be included for consistency at this order [32]. In the rough numerical analysis we do later on, we will treat the contributions from these coefficients as part of the uncertainty.

Note that in deriving the result in Eq. (25) we have dropped $i\epsilon$ factors from the propagators. If these terms were kept, the second term in $F(x,y)$ would be

$$\frac{1}{(y+i\epsilon)(x\bar{y}-1+i\epsilon)}. \tag{31}$$

The $i\epsilon$'s yield imaginary contributions with $\delta(y)$ and $\delta(x\bar{y}-1)$. They contribute for $y = 0$ or for $x = \bar{y} = 1$, so these contributions occur in zero bins, which are excluded from the convolution integrals in the factorization theorem we have derived with SCET. The zero bins correspond to degrees of freedom that are soft, and including these regions would induce a double counting, so the correct factorization theorem in QCD does not include them. Factors analogous to $x \neq 0$ and $x' \neq 0$ in Eq. (27) ensure that there is no contribution to the integral from any zero-bin momentum, and we find that the δ-function terms give zero. This remains true for more singular distributions yielding $\delta^{(n)}(x)$, and so also applies to the first term in $F(x,y)$. Thus it is correct to drop the $i\epsilon$ factors from the start. This should be compared with the approach in KLS where the $i\epsilon$ factors generate a strong phase from the tree-level diagrams from a $k_\perp^2$ dependent δ function. In our derivation any such $k_\perp^2$ imaginary terms could only occur at higher orders in Λ/m_b.

Thus at order $\alpha_s(\mu_h)$ the lowest order annihilation factorization theorem is determined by the convolutions

$$\begin{aligned}
&\int_0^1 dxdyF(x,y)\phi^{M_1}(y)\phi^{M_2}(x)\\
&\quad=\langle\bar{x}^{-2}\rangle^{M_2}\langle y^{-1}\rangle^{M_1}-\langle[y(x\bar{y}-1)]^{-1}\rangle^{M_1M_2}\\
&\qquad+d(\mu_-)\phi'_{M_2}(1)\langle y^{-1}\rangle^{M_1},\\
&\int_0^1 dxdyF(\bar{y},\bar{x})\phi^{M_1}(y)\phi^{M_2}(x)\\
&\quad=\langle y^{-2}\rangle^{M_1}\langle\bar{x}^{-1}\rangle^{M_2}-\langle[\bar{x}(x\bar{y}-1)]^{-1}\rangle^{M_1M_2}\\
&\qquad-d(\mu_+)\phi'_{M_1}(0)\langle\bar{x}^{-1}\rangle^{M_2}.
\end{aligned}\tag{32}$$

Here we use Eq. (29), and

$$\begin{aligned}
\langle y^{-1}\rangle^M&=\int_0^1 dy\,\frac{\phi^M(y,\mu)}{y},\\
\langle f(x,y)\rangle^{M_1M_2}&=\int_0^1 dx\int_0^1 dy f(x,y)\\
&\quad\times\phi^{M_1}(y,\mu)\phi^{M_2}(x,\mu).
\end{aligned}\tag{33}$$

These results do not have a complex phase because the right-hand side of Eq. (32) is real.

We have shown that the convolution formula in Eq. (23) for the local contributions $O_i^{(1L)}$ yields a well-defined annihilation amplitude. At order $\alpha_s(m_b)$ the result is real, so $A_{\rm Lann}^{(1)}$ is real up to perturbative corrections. Order $\alpha_s^2(m_b)$ corrections to the a_i will produce perturbative strong phases in $A_{\rm Lann}^{(1)}$. Further discussion on strong phases is given in Sec. V, while phenomenological implications are taken up in Sec. VI.

IV. CHIRALLY ENHANCED LOCAL ANNIHILATION CONTRIBUTIONS

At order $\alpha_s(\mu_h)\mu_M\Lambda/m_b^2$ there are contributions from chirally enhanced operators that could compete with the $\alpha_s(\mu_h)\Lambda/m_b$ terms [10]. In SCET we define these contributions as the set of $\mathrm{SCET_{II}}$ operators analogous to $O_i^{(1L)}$ but with an extra $\not{\mathcal{P}}_\perp$ between collinear quark fields. We start by constructing a complete basis for local operators at this order with a $\mathcal{P}_\perp^\beta$, calling them $O_i^{(2L)}$. These operators have the same color and flavor structures as Eq. (17). The chiral structures induced from the operators O_{1-10} and the initial basis of Dirac structures shown in Eq. (13) are also the same, and allow us to eliminate many possibilities.

The complete set of Dirac structures from matching the operators $O_{1-4,9,10}$ include

$$\begin{aligned}
\Gamma_s\otimes\Gamma_{\bar n}\otimes\Gamma_n\mathcal{P}_\perp^\beta=\{&\gamma_\beta^\perp\otimes\not{n}\otimes\not{\bar n}\mathcal{P}_\perp^\beta,\ \gamma_\perp^\alpha\otimes\not{n}\gamma_\alpha^\perp\otimes\not{\bar n}\gamma_\beta^\perp\mathcal{P}_\perp^\beta,\\
&\gamma_\beta^\perp\otimes\not{n}\gamma_\perp^\alpha\otimes\not{\bar n}\gamma_\alpha^\perp\mathcal{P}_\perp^\beta,\\
&\gamma_\perp^\alpha\otimes\not{n}\gamma_\beta^\perp\otimes\not{\bar n}\gamma_\alpha^\perp\mathcal{P}_\perp^\beta\},
\end{aligned}\tag{34}$$

plus the analogous set $\Gamma_s\otimes\Gamma_{\bar n}\mathcal{P}_\perp^\beta\otimes\Gamma_n$. Our basis does not include operators with $\mathcal{P}_\perp^\dagger$, because the mesons M_i have zero $\perp$ -momenta, so we can integrate these terms by parts to put them in the form in Eq. (34). The third term in Eq. (34) has chiral structure $(LH)(LR)(RL)$ and vanishes by Eq. (14). The terms in Eq. (34) all have $\bar q_s\gamma_\perp^\mu b_v$, and so do not contribute for B decays. The same holds if we replace $\mathcal{P}_\perp^\beta$ by $ig\mathcal{B}_\perp^\beta$. Thus, at any order in perturbation theory the only $\mathcal{O}(\eta^8)$ local operator contributions from $O_{1-4,9,10}$ are those with a D_s^μ in the soft bilinear.

For O_{5-8} we have the structures in Eq. (34), and when the q' flavor is a soft quark with $P_L\otimes P_R$ Dirac structure from O_i, we also have

$$\begin{aligned}
\Gamma_s\otimes\Gamma_{\bar n}\otimes\Gamma_n\mathcal{P}_\perp^\beta&=\{1\otimes\not{n}\otimes\not{\bar n}\not{\mathcal{P}}_\perp,\ 1\otimes\not{n}\gamma_\beta^\perp\otimes\not{\bar n}\mathcal{P}_\perp^\beta\},\\
\Gamma_s\otimes\Gamma_{\bar n}\mathcal{P}_\perp^\beta\otimes\Gamma_n&=\{1\otimes\not{n}\mathcal{P}_\perp^\beta\otimes\not{\bar n}\gamma_\beta^\perp,\ 1\otimes\not{n}\not{\mathcal{P}}_\perp\otimes\not{\bar n}\},
\end{aligned}\tag{35}$$

plus operators with 1 replaced by $\not{\bar n}-\not{n}$, which vanish due to Eq. (16). The operators in Eq. (35) contribute to B decays. In particular, they yield both transverse and longitudinal polarization in $B\to VV$. A complete basis for the local $\mathcal{O}(\eta^8)$ operators with one $\mathcal{P}_\perp^\beta$ is

$$\begin{aligned}
O_{1d}^{(2L)}&=\frac{1}{m_b^4}\sum_{q,q'}[\bar q_s' P_L b_v][\bar d_{\bar n,\omega_2}\not{n}P_L q_{\bar n,\omega_3}][\bar q_{n,\omega_1}\not{\bar n}\not{\mathcal{P}}_\perp P_R q'_{n,\omega_4}],\\
O_{2d}^{(2L)}&=\frac{1}{m_b^4}\sum_{q,q'}[\bar q_s' P_L b_v][\bar d_{\bar n,\omega_2}\not{n}\not{\mathcal{P}}_\perp P_R q_{\bar n,\omega_3}][\bar q_{n,\omega_1}\not{\bar n}P_R q'_{n,\omega_4}],\\
O_{3d}^{(2L)}&=\frac{1}{m_b^4}\sum_{q,q'}[\bar q_s' P_L b_v][\bar d_{\bar n,\omega_2}\not{n}\gamma_\beta^\perp P_R q_{\bar n,\omega_3}][\bar q_{n,\omega_1}\not{\bar n}P_R\mathcal{P}_\perp^\beta q'_{n,\omega_4}],\\
O_{4d}^{(2L)}&=\frac{1}{m_b^4}\sum_{q,q'}[\bar q_s' P_L b_v][\bar d_{\bar n,\omega_2}\not{n}P_L\mathcal{P}_\perp^\beta q_{\bar n,\omega_3}][\bar q_{n,\omega_1}\not{\bar n}\gamma_\beta^\perp P_R q'_{n,\omega_4}],\qquad O_{5d-8d}^{(2L)}=O_{1d-4d}^{(2L)}\frac{3e_{q'}}{2},
\end{aligned}\tag{36}$$

with sums over q, $q'=u,d,s$. Note that the flavor structure of these operators is identical to $O_{4d}^{(1L)}$. For the electroweak penguin operators $O_{7,8}$ an additional four operators $O_{5d-8d}^{(2L)}$ are needed, which have the same spin-flavor structures as $O_{1d-4d}^{(2L)}$, but with an $e_{q'}$ charge factor, $\sum_{q,q'}3e_{q'}/2$. Again we caution that we have not considered the complete set of local Λ^2/m_b^2 operators, since our basis does not include three-body terms with an $ig\mathcal{B}_\perp^\mu$, nor terms with an extra D_s soft covariant derivative. We have also not considered $\mathcal{O}(\mu_{M_1}\mu_{M_2}\Lambda/m_b^3)$ terms. All these terms are

real, and it would be interesting to calculate them in the future.

The weak Hamiltonian with Wilson coefficients for the operators $O_{id}^{(2L)}$ is

$$H_W = \frac{4G_F}{\sqrt{2}}(\lambda_u^{(d)} + \lambda_c^{(d)})\sum_{n,\bar{n}}\int[d\omega_1 d\omega_2 d\omega_3 d\omega_4]\sum_{i=1-8} a_i^{\chi}(\omega_j)O_{id}^{(2L)}(\omega_j). \tag{37}$$

Since only the penguin operators O_{5-8} contribute, we pulled out the common CKM factor. Matching at tree level onto the operators $O_{id}^{(2L)}$ by keeping terms linear in the $\perp$ -momenta in Fig. 2, we find

$$\begin{aligned}
a_1^{\chi}(x,y) &= \frac{4C_F\pi\alpha_s(\mu_h)}{N_c}\left[\left(C_6+\frac{C_5}{N_c}\right)F_1(x,y)+\frac{C_5}{N_c}F_2(x,y)\right]_{\oslash},\\
a_2^{\chi}(x,y) &= \frac{4C_F\pi\alpha_s(\mu_h)}{N_c}\left[-\left(C_6+\frac{C_5}{N_c}\right)F_1(\bar{y},\bar{x})+\frac{C_5}{N_c}F_2(\bar{y},\bar{x})\right]_{\oslash},\\
a_3^{\chi}(x,y) &= \frac{4C_F\pi\alpha_s(\mu_h)}{N_c}\left[-\left(C_6+\frac{C_5}{N_c}\right)F_3(x,y)-\frac{C_5}{N_c}F_2(x,y)\right]_{\oslash},\\
a_4^{\chi}(x,y) &= \frac{4C_F\pi\alpha_s(\mu_h)}{N_c}\left[\left(C_6+\frac{C_5}{N_c}\right)F_3(x,y)-\frac{C_5}{N_c}F_2(\bar{y},\bar{x})\right]_{\oslash},\\
a_{5-8}^{\chi}(x,y) &= a_{1-4}^{\chi}(x,y) \quad \text{with } C_5\to C_7,\ C_6\to C_8,
\end{aligned} \tag{38}$$

where x and y are defined in Fig. 2 and

$$\begin{aligned}
F_1(x,y) &= \left[\frac{1+\bar{x}}{y^2\bar{y}\bar{x}^2}\right]_{\oslash} + d_1(\mu_-)\delta'(\bar{x})\left[\frac{1}{y^2\bar{y}}\right]_{\oslash}\\
&\quad + d_2(\mu_+)\delta'(y)\left[\frac{1+\bar{x}}{\bar{x}^2}\right]_{\oslash} + d_3(\mu_\pm)\delta'(\bar{x})\delta'(y),\\
F_2(x,y) &= \left[\frac{1}{(1-x\bar{y})\bar{x}y^2}\right]_{\oslash},\\
F_3(x,y) &= \left[\frac{1}{y^2\bar{x}^2}\right]_{\oslash} + d_4(\mu_-)\delta'(\bar{x})\left[\frac{1}{y^2}\right]_{\oslash}\\
&\quad + d_5(\mu_+)\delta'(y)\left[\frac{1}{\bar{x}^2}\right]_{\oslash} + d_6(\mu_\pm)\delta'(\bar{x})\delta'(y).
\end{aligned} \tag{39}$$

Here d_{1-6} play the same role as d in Eq. (25). The coefficients a_{1-8}^{χ} are polluted in the sense of Ref. [5], meaning that $\mathcal{O}(\alpha_s^2)$ matching results proportional to the large coefficients $C_{1,2}$ could compete numerically. This makes the computation of these $\mathcal{O}(\alpha_s^2)$ corrections important.

For decays involving a pseudoscalar in the final state, the operators $O_{1d}^{(2L)}$ and $O_{2d}^{(2L)}$ generate so-called "chirally enhanced" terms, proportional to μ_M. Time-ordered products of SCET$_{\rm I}$ operators also generate μ_M terms, but only at $\mathcal{O}(\alpha_s^2)$. It is not clear that the chirally enhanced terms are larger numerically than other power corrections. In particular, three-body distributions from operators with $\bar{\xi}_n(ig\mathcal{B}_\perp^\mu)\Gamma\xi_n$ are parametrically (and sometimes numerically as well) of similar importance [33]. The distributions are related by [34]

$$\begin{aligned}
&f_P\mu_P\left[\phi_\sigma^{P\prime}(x)+\frac{(2x-1)}{x(1-x)}\phi_\sigma^P(x)\right]\\
&\quad = -6f_{3P}\left[\frac{G_{P_z}^{(t)}(x)}{x}+\frac{G_{P_y}^{(t)}(x)}{1-x}\right],\\
&f_P\mu_P\left[\phi_p^P(x)-\frac{1}{6x(1-x)}\phi_\sigma^P(x)\right]\\
&\quad = -f_{3P}\left[\frac{G_{P_z}^{(t)}(x)}{x}-\frac{G_{P_y}^{(t)}(x)}{1-x}\right],
\end{aligned} \tag{40}$$

where $G_{P_z}^{(t)}(x)$ and $G_{P_y}^{(t)}(x)$ are integrals over the three-parton distribution, ϕ_{3P}. These relations allow certain chirally enhanced terms with $\mu_P f_P$ to be traded for nonchirally enhanced terms with f_{3P}. Thus it is clear that the chirally enhanced terms dominate over the three-body operators only in the special case when the linear combinations in the square brackets on the left-hand side of Eq. (40) are numerically suppressed. Solving with these linear combinations set to zero determines the two-body distributions ϕ_σ^P and ϕ_p^P in the Wandzura-Wilczek (WW) approximation [35]. Thus in order to uniquely specify the μ_P dependent terms, the WW approximation was needed in Ref. [10].

In contrast, in SCET we are not forced to assume a numerical dominance of the μ_P terms to uniquely identify them. We can instead define local chirally enhanced annihilation terms to be the matrix elements of the operators $O_{1d}^{(2L)}$ and $O_{2d}^{(2L)}$ for final states with a pseudoscalar. With a minimal basis of operators, the matrix elements of these terms are unique. The remaining terms involve other operators, and we postpone discussing them to future work.

We proceed to work out the factorization formula for $O_{1d}^{(2L)}$ and $O_{2d}^{(2L)}$ with steps analogous to Eqs. (20)–(23). To take the matrix element we need Eq. (21) and the result

$$\langle P_{n_1}(p)|\bar{q}^{(f)}_{n,\omega}\, \not{n}\, \not{\mathcal{P}}_\perp P_R q^{(f')}_{n,\omega'}|0\rangle = -\frac{i}{6} c_{Pff'}\delta_{nn_1}\delta(\bar{n}\cdot p-\omega+\omega') \times f_P \mu_P \phi^P_{pp}(y). \quad (41)$$

Here $c_{Pff'}$ are Clebsch-Gordan factors, $y=\omega/\bar{n}\cdot p$, and we have not written the ω' dependence in the distribution due to the δ function. The distribution $\phi^P_{pp}(y)$ is related to more standard twist-3 two-parton and three-parton distributions by [18,34]

$$\phi^P_{pp}(y) = 3y\Big[\phi^P_p(y)+\frac{1}{6}\phi^{P\prime}_\sigma(y) + \frac{2f_{3P}}{f_P\mu_P}\int\frac{dy'}{y'}\phi_{3P}(y-y',y)\Big]. \quad (42)$$

Note that in $\mu_P\phi^P_{pp}$, the ϕ_{3P} term does not have the chiral enhancement factor μ_P. There will be additional terms proportional to ϕ_{3P} generated by three-body operators. We choose the ϕ^P_{pp} and ϕ_{3P} basis of twist-3 distributions, keeping in mind the relations in Eq. (40). For decays involving one or more pseudoscalars in the final state, we find the chirally enhanced local annihilation amplitudes

$$A^{(2)}_{\rm Lann} = -\frac{G_F f_B f_{M_1} f_{M_2}}{6\sqrt{2}m_b}(\lambda_u^{(d)}+\lambda_c^{(d)}) \times\int_0^1 dxdy[\mu_{M_1}H_{\chi 1}(x,y)\phi^{M_1}_{pp}(y)\phi^{M_2}(x) + \mu_{M_2}H_{\chi 2}(x,y)\phi^{M_1}(y)\phi^{M_2}_{pp}(x)], \quad (43)$$

where $\mu_\rho=\mu_{K^*}=0$ and using isospin $\mu_\pi = m_\pi^2/(m_u+m_d)$, $\mu_K = m_K^2/(m_s+m_u) = m_K^2/(m_s+m_d)$. Terms with ϕ_{3P} or terms of the same order with a D_s^μ in their soft matrix elements have not been included in our $A^{(2)}_{\rm Lann}$, though they also give local annihilation contributions to $A^{(2)}$. Furthermore, we focused on the pseudoscalar matrix element in Eq. (41) to derive the contribution in Eq. (43). The $O^{(2L)}_{1d,2d}$ operators in Eq. (36) will contribute additional terms for decays to longitudinal vector mesons involving distributions $h_\parallel^{(s)\prime}$ and $h_\parallel^{(t)}$ (our notation for these distributions follows Ref. [34]). The operators $O^{(2L)}_{3d,4d}$ will produce decays to two transverse vectors with distributions from among $\phi_\perp$, F, $\mathcal{V}$, $\mathcal{A}$. It would be straightforward to work out a factorization theorem from the operators $O^{(2L)}_{id}$ in terms of these distributions, though we will not do so here.

Results for the hard coefficients $H_{\chi 1}$ and $H_{\chi 2}$ in terms of the Wilson coefficients a_i^χ are given in Table IV for $\bar{B}^0$ and B^- decays and in Table V for $\bar{B}_s$ decays. Note that there are no chirally enhanced annihilation contributions for the $\bar{B}_s\to\pi\pi$ or $\bar{B}_s\to\rho\pi$ channels, so B_s decays could potentially be used to separate annihilation contributions from $A^{(1)}_{\rm Lann}$ and $A^{(2)}_{\rm Lann}$. For later convenience we define moment parameters

$$\beta^{M_1M_2}_{\chi 1,\chi 5} = \frac{1}{6}\int_0^1 dxdy a^\chi_{1,5}(x,y)\phi^{M_1}_{pp}(y)\phi^{M_2}(x),$$
$$\beta^{M_1M_2}_{\chi 2,\chi 6} = \frac{1}{6}\int_0^1 dxdy a^\chi_{2,6}(x,y)\phi^{M_1}(y)\phi^{M_2}_{pp}(x). \quad (44)$$

Neglecting ϕ_{3P} in the WW approximation yields $\phi^P_{pp}(y)=6y(1-y)$. At order $\alpha_s(\mu_h)$ our results for $\beta_{\chi 1}$ and $\beta_{\chi 2}$, taken with the WW approximation, agree with the convolutions derived in this limit in Refs. [10,11]. Ignoring the ϕ distributions we would find that these convolution integrals diverge. The zero bin avoided double counting in our convolutions, and yields a finite and real result for the chirally enhanced annihilation amplitude.

TABLE IV. Hard functions for the annihilation amplitude $A^{(2)}_{\rm Lann}$ in Eq. (43) for $\bar{B}^0$ and B^- decays. The result for $B^-\to\pi^0\pi^-$ is obtained by adding the results using the entries from the first two rows, and so vanishes in the isospin limit.

M_1M_2	$H_{\chi 1}(x,y)$	$H_{\chi 2}(x,y)$
$\pi^0\pi^-$, $\rho^0\pi^-$ $\pi^0\rho^-$	$-\frac{1}{\sqrt{2}}a_1^\chi(x,y)-\frac{1}{\sqrt{2}}a_5^\chi(x,y)$	$\frac{1}{\sqrt{2}}a_2^\chi(x,y)+\frac{1}{\sqrt{2}}a_6^\chi(x,y)$
$\pi^-\pi^0$, $\rho^-\pi^0$ $\pi^-\rho^0$	$\frac{1}{\sqrt{2}}a_1^\chi(x,y)+\frac{1}{\sqrt{2}}a_5^\chi(x,y)$	$-\frac{1}{\sqrt{2}}a_2^\chi(x,y)-\frac{1}{\sqrt{2}}a_6^\chi(x,y)$
$\pi^+\pi^-$, $\pi^+\rho^-$, $\rho^+\pi^-$	$-a_1^\chi(x,y)+\frac{1}{2}a_5^\chi(x,y)$	$a_2^\chi(x,y)-\frac{1}{2}a_6^\chi(x,y)$
$\pi^0\pi^0$, $\rho^+K^{(*)-}$, $\rho^0\pi^0$	$a_1^\chi(x,y)-\frac{1}{2}a_5^\chi(x,y)$	$-a_2^\chi(x,y)+\frac{1}{2}a_6^\chi(x,y)$
$K^-K^{(*)+}$, $K^{(*)-}K^+$	⋯	⋯
$\bar{K}^0K^{(*)0}$, $\bar{K}^{(*)0}K^0$	$a_1^\chi(x,y)-\frac{1}{2}a_5^\chi(x,y)$	$-a_2^\chi(x,y)+\frac{1}{2}a_6^\chi(x,y)$
$K^-K^{(*)0}$, $K^{(*)-}K^0$	$a_1^\chi(x,y)+a_5^\chi(x,y)$	$-a_2^\chi(x,y)-a_6^\chi(x,y)$
$\pi^-\bar{K}^{(*)0}$, $\rho^-\bar{K}^0$	$a_1^\chi(x,y)+a_5^\chi(x,y)$	$-a_2^\chi(x,y)-a_6^\chi(x,y)$
$\pi^0K^{(*)-}$, ρ^0K^-	$-\frac{1}{\sqrt{2}}a_1^\chi(x,y)-\frac{1}{\sqrt{2}}a_5^\chi(x,y)$	$\frac{1}{\sqrt{2}}a_2^\chi(x,y)+\frac{1}{\sqrt{2}}a_6^\chi(x,y)$
$\pi^0\bar{K}^{(*)0}$, $\rho^0\bar{K}^0$	$\frac{1}{\sqrt{2}}a_1^\chi(x,y)-\frac{1}{2\sqrt{2}}a_5^\chi(x,y)$	$-\frac{1}{\sqrt{2}}a_2^\chi(x,y)+\frac{1}{2\sqrt{2}}a_6^\chi(x,y)$
$\pi^+K^{(*)-}$, ρ^+K^-	$-a_1^\chi(x,y)+\frac{1}{2}a_5^\chi(x,y)$	$a_2^\chi(x,y)-\frac{1}{2}a_6^\chi(x,y)$

TABLE V. Hard functions for the annihilation amplitude $A^{(2)}_{\rm Lann}$ in Eq. (43) for $\bar{B}_s$ decays.

M_1M_2	$H_{\chi 1}(x,y)$	$H_{\chi 2}(x,y)$
$K^+\pi^-$, $K^{*+}\pi^-$, $K^+\rho^-$	$-a_1^\chi(x,y)+\frac{1}{2}a_5^\chi(x,y)$	$a_2^\chi(x,y)-\frac{1}{2}a_6^\chi(x,y)$
$K^0\pi^0$, $K^{*0}\pi^0$, $K^0\rho^0$	$\frac{1}{\sqrt{2}}a_1^\chi(x,y)-\frac{1}{2\sqrt{2}}a_5^\chi(x,y)$	$-\frac{1}{\sqrt{2}}a_2^\chi(x,y)+\frac{1}{2\sqrt{2}}a_6^\chi(x,y)$
K^+K^-, $K^{*+}K^-$, K^+K^{*-}	$-a_1^\chi(x,y)+\frac{1}{2}a_5^\chi(x,y)$	$a_2^\chi(x,y)-\frac{1}{2}a_6^\chi(x,y)$
$K^0\bar{K}^0$, $K^{*0}\bar{K}^0$, $K^0\bar{K}^{*0}$	$a_1^\chi(x,y)-\frac{1}{2}a_5^\chi(x,y)$	$-a_2^\chi(x,y)+\frac{1}{2}a_6^\chi(x,y)$

Let us see how the convolutions work out at order $\alpha_s(\mu_h)$ following Ref. [18]. We need two standard convolutions involving zero-bin subtractions,

$$\begin{aligned}&\int_0^1 dxdy\left[\frac{1+\bar{x}}{y^2\bar{y}\bar{x}^2}\right]_\phi \phi_{pp}^{M_1}(y)\phi^{M_2}(x)\\&\quad=\langle y^{-2}\bar{y}^{-1}\rangle_{pp}^{M_1}(\langle\bar{x}^{-2}\rangle^{M_2}+\langle\bar{x}^{-1}\rangle^{M_2}),\\&\int_0^1 dxdy\left[\frac{1+y}{y^2x\bar{x}^2}\right]_\phi \phi^{M_1}(y)\phi_{pp}^{M_2}(x)\\&\quad=\langle\bar{x}^{-2}x^{-1}\rangle_{pp}^{M_2}(\langle y^{-2}\rangle^{M_1}+\langle y^{-1}\rangle^{M_1}).\end{aligned}\tag{45}$$

Here we model the y^{-2}, y^{-1} moments as in Eqs. (29) and (33), and for the remaining convolution we again assume there is no interference between the rapidity renormalization and invariant mass renormalization to find

$$\begin{aligned}\langle y^{-2}\bar{y}^{-1}\rangle_{pp}^{M_1}=&\int_0^1 dy\left[\frac{\phi_{pp}^{M_1}(y,\mu)}{y^2(1-y)}-\frac{y\phi_{pp}^{M_1\prime}(0,\mu)}{y^2}\right]\\&+\phi_{pp}^{M_1\prime}(0,\mu)\ln\left(\frac{n\cdot p_{M_1}}{\mu_+}\right).\end{aligned}\tag{46}$$

The $\mu_\pm$ dependence is canceled by tree-level logarithmic dependence in the coefficients, $d_{1,4}(\mu_-)=\ln(p_M^-/\mu_-)$, $d_{2,5}(\mu_+)=\ln(p_M^+/\mu_+)$, $d_{3,6}(\mu_\pm)=\ln(p_M^-/\mu_-)\times\ln(p_M^+/\mu_+)$. The kernels in Eq. (38) also involve two more complicated convolutions that are derived in the Appendix,

$$\begin{aligned}\langle[(1-x\bar{y})\bar{x}y^2]^{-1}\rangle_{pp}^{M_1M_2}=&\int_0^1 dxdy\left[\frac{1}{(1-x\bar{y})\bar{x}y^2}\right]_\phi\phi_{pp}^{M_1}(y)\phi^{M_2}(x)\\=&\int_0^1 dx\int_0^1 dy\left[\frac{\phi_{pp}^{M_1}(y)\phi^{M_2}(x)}{(\bar{x}+y-\bar{x}y)\bar{x}y^2}-\frac{\phi_{pp}^{M_1\prime}(0)\phi^{M_2}(x)}{(\bar{x}+y)\bar{x}y}\right]-\phi_{pp}^{M_1\prime}(0)\int_0^1 dx\frac{\phi^{M_2}(x)\ln(2-x)}{(1-x)^2},\\\langle[(1-x\bar{y})\bar{x}^2y]^{-1}\rangle_{pp}^{M_2M_1}=&\int_0^1 dxdy\left[\frac{1}{(1-x\bar{y})\bar{x}^2y}\right]_\phi\phi^{M_1}(y)\phi_{pp}^{M_2}(x)\\=&\int_0^1 dy\int_0^1 dx\left[\frac{\phi^{M_1}(y)\phi_{pp}^{M_2}(x)}{(\bar{x}+y-\bar{x}y)\bar{x}^2y}+\frac{\phi^{M_1}(y)\phi_{pp}^{M_2\prime}(1)}{(\bar{x}+y)\bar{x}y}\right]+\phi_{pp}^{M_2\prime}(1)\int_0^1 dy\frac{\phi^{M_1}(y)\ln(1+y)}{y^2}.\end{aligned}\tag{47}$$

As promised, the minimal subtraction scheme yields a well-defined result for $A^{(2)}_{\rm Lann}$. The scheme dependence cancels order by order in α_s between the matrix element and perturbative corrections to the kernels obtained by matching. In any scheme the result at order $\alpha_s(\mu_h)$ is real.

V. GENERATING STRONG PHASES

In this section we derive results for the order at which strong phases occur in the power suppressed amplitudes $A^{(1)}$. It is convenient to classify complex contributions to the $B\to M_1M_2$ amplitudes according to the distance scale at which they are generated. We use the terminology hard, jet, and nonperturbative to refer to imaginary contributions from the scales m_b, $\sqrt{m_b\Lambda}$, and Λ^2, respectively. We will not attempt to classify strong phases generated by charm loops, since a complete understanding of factorization for these terms order by order in a power counting expansion is not yet available.

For a matrix element to have a physical complex phase it must contain information about both final state mesons. Generically, terms in the factorized power expansion of $B\to M_1M_2$ amplitudes involve only vacuum to meson matrix elements, so strong phase information can be contained in the Wilson coefficients or the factorized operators, but not in the states. This provides tight constraints on the source of strong phases. Nonperturbative strong phases will occur if matrix elements of these factorized operators give complex distribution functions. A sufficient condition to generate a nonperturbative phase is to have a factorized operator that is sensitive to the directions of two or more final state mesons [3], information that can be carried by Wilson lines. Physically, this is a manifestation of soft rescattering of final states. In processes like ours where soft-collinear and collinear (n)-collinear ($\bar{n}$) factorization are relevant, and there is only one hadron in any given light-cone direction, this criterion implies that all strong phases reside in the soft matrix elements, where the direc-

tional information from collinear hadrons is retained in soft Wilson lines, S_r, with direction r^μ. Since $S_r^\dagger S_r = 1$ these Wilson lines often cancel, but for many of the power suppressed terms listed in Table I the cancellation is not complete. This mechanism for generating a strong phase was first observed for $\bar{B}^0 \to D^0\pi^0$ [3], where a nonperturbative soft matrix element occurs through four-quark operators depending on n and v' (which are null and timelike vectors for the final state light and charmed mesons, respectively).

For the $B \to M_1 M_2$ decays with two energetic light mesons, a nonperturbative strong phase requires a soft matrix element depending on the S_n and $S_{\bar{n}}$ Wilson lines in $\mathrm{SCET_{II}}$. The simplest way to obtain the Wilson lines for the soft operators is to match $\mathrm{SCET_I}$ onto $\mathrm{SCET_{II}}$ [27]. In $\mathrm{SCET_I}$ one first uses the decoupling field redefinition on collinear fields [16], $\xi_n \to Y_n \xi_n$, $\xi_{\bar{n}} \to Y_{\bar{n}} \xi_{\bar{n}}$, $A_n \to Y_n A_n Y_n^\dagger$, and $A_{\bar{n}} \to Y_{\bar{n}} A_{\bar{n}} Y_{\bar{n}}^\dagger$, which generates the Wilson lines and factorizes usoft and collinear fields. The fields of a given type are then grouped together by Fierz rearrangements. Matching the resulting operators or time-ordered products onto $\mathrm{SCET_{II}}$ gives $Y_r \to S_r$, and we can read off which soft Wilson lines are present. Because of the properties of the subleading $\mathrm{SCET_I}$ operators, we will not have an S_n and $S_{\bar{n}}$ in the final $\mathrm{SCET_{II}}$ operator unless we have a subleading $\mathrm{SCET_I}$ Lagrangian with an n-collinear field and usoft fields, and one with $\bar{n}$-collinear fields and usoft fields. We used this property to determine which entries are real or complex, and listed the results in the last column of Table I. The complex entries with multiple $\mathcal{L}_{\xi q}^{(j)}$'s [36] also have at least two hard-collinear gluons, and so generate contributions that start at $\alpha_s(\mu_i)^2$ when matched onto $\mathrm{SCET_{II}}$.

To determine the perturbative order of the complex contributions, we must also classify which hard and jet coefficients give complex phases. In general, any hard coefficient generated by matching at ≥ 1 loop will give imaginary contributions, since these loops involve fields for both final state mesons, as pointed out for the general case in Ref. [2] and for charm loops in Ref. [37]. Since all leading order contributions in Table I have at least one $\alpha_s(\mu_i)$, the hard imaginary contributions for $A^{(0)}$ are $\mathcal{O}[\alpha_s(\mu_i)\alpha_s(\mu_h)/\pi]$. At order Λ/m_b all annihilation contributions but $Q_i^{(4)}$ have at least one $\alpha_s(\mu_i)$, and for these terms the hard complex contributions involve $\alpha_s(\mu_i)\alpha_s(\mu_h)$ and thus are smaller than the nonperturbative terms proportional to $\alpha_s(\mu_i)^2$. For $Q_i^{(4)}$ the amplitude is real at the leading perturbative order, $\alpha_s(\mu_h)$, as demonstrated in Sec. III, and so hard complex contributions start at $\alpha_s^2(\mu_h)$. In contrast, for the amplitude $A_{\mathrm{rest}}^{(1)}$ a complex amplitude is generated at order $\alpha_s(\mu_i)\Lambda/m_b$, which is only suppressed by Λ/m_b compared to $A^{(0)}$.

Finally, we should examine complex contributions from the jet scale. At leading order there is a unique jet function J [5]. J also contributes to the heavy-to-light form factors and only knows about the n-collinear direction. Thus $A^{(0)}$ does not get imaginary contributions at any order in the $\alpha_s(\mu_i)$ expansion (which has been demonstrated explicitly to $\alpha_s^2(\mu_i)$ [38]). At next-to-leading order in the power expansion, there is no known relation of the power suppressed jet functions with analogous jet functions in the form factors. However, the subleading jet functions also depend only on one collinear direction, and do not carry information about both final state mesons that could generate a physical strong phase. We demonstrate this fact more explicitly by examining the calculation at $\mathcal{O}(\alpha_s(\mu_i))$, which is sufficient to see that the amplitudes are real up to the order where a nonperturbative phase first occurs. At this order the jet functions are generated by matching tree-level $\mathrm{SCET_I}$ diagrams onto $\mathrm{SCET_{II}}$. A typical example is

$$\frac{1}{(x + i\epsilon)(k^+ + i\epsilon)}, \tag{48}$$

where x is a momentum fraction that will be convolved with a collinear distribution function, and the k^+ will be convolved with a soft distribution function. These jet functions are real if and only if we can drop the $i\epsilon$ factors. However, just as in Sec. III, the $i\epsilon$ terms can be dropped because the zero-bin subtractions [18] ensure that this does not change the convolution.[4] Thus factorization gives real $\mathcal{O}(\alpha_s(\mu_i))$ jet functions.

This demonstrates that complex contributions in the power suppressed annihilation amplitudes are suppressed,

$$\mathrm{Im}\left[\frac{A_{\mathrm{ann}}^{(1)}}{A^{(0)}}\right] = \mathcal{O}\left(\frac{\alpha_s(\mu_i)}{\pi}\frac{\Lambda}{m_b}\right) + \mathcal{O}\left(\frac{\Lambda^2}{m_b^2}\right). \tag{49}$$

On general grounds one might have expected $\mathcal{O}(\Lambda/m_b)$ suppressed strong phases, which we have demonstrated are absent in $A_{\mathrm{ann}}^{(1)}$, though they do occur in $A_{\mathrm{rest}}^{(1)}$.

We close this section by giving two examples of time-ordered products generating the nonperturbative strong phases discussed above. We consider a time-ordered product with three $\mathcal{L}_{\xi q}^{(1)}$ insertions contributing to annihilation. When matching onto $\mathrm{SCET_{II}}$ we integrate out the hard-collinear modes, leading to an eight-quark operator. Figure 3(a) shows the order $\alpha_s^2(\mu_i)$ contribution to this matching. The soft quark lines remain open as their contraction leads to an on-shell line which must be treated nonperturbatively. The resulting $\mathrm{SCET_{II}}$ operator has the generic form

$$\begin{aligned} O^{\mathrm{II}} = {} & J(n_2\cdot p, n_1\cdot l, n_1\cdot r, n_2\cdot q, n_1\cdot k) \\ & \times (\bar{q}_s S_{n_1})_{n_1\cdot r}\Gamma^{(1)}(S_{n_2}^\dagger q_s)_{n_2\cdot q}(\bar{q}_s S_{n_2})_{n_1\cdot k}\Gamma^{(2)}(S_{n_1}^\dagger h_v) \\ & \times (\bar{q}_{n_1,l}\Gamma^{(3)} q_{n_1,l'})(\bar{q}_{n_2,p'}\Gamma^{(4)} q_{n_2,p}) \end{aligned} \tag{50}$$

[4] An equivalent physical argument for dropping the $i\epsilon$ factors was given in Ref. [3] to demonstrate that certain long-distance contributions are absent in color suppressed decays.

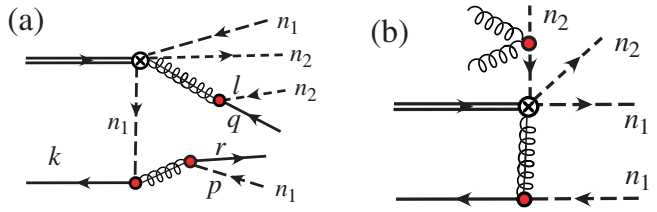

FIG. 3 (color online). Graphs which generate a strong phase in lowest order matching of $\mathrm{SCET_I}$ operators onto $\mathrm{SCET_{II}}$: (a) has a $Q^{(1)}$, two $\mathcal{L}^{(1)}_{\xi_{n_1} q}$, and one $\mathcal{L}^{(1)}_{\xi_{n_2} q}$ and contributes to the annihilation amplitude at $\mathcal{O}(\alpha_s^2(\mu_i))$; and (b) has a $Q^{(1)}$, one $\mathcal{L}^{(1)}_{\xi_{n_1} q}$, and one $\mathcal{L}^{(2)}_{\xi_{n_2}\xi_{n_2}}$ and contributes to nonannihilation amplitudes at $\mathcal{O}(\alpha_s(\mu_i))$. Dashed quark lines are n_1 or n_2 collinear, and solid quark lines are soft.

where we use the shorthand subscript notation, $(S^\dagger_{n_i} q_s)_{n_i\cdot q} \equiv [\delta(n_i\cdot q - n_i\cdot\mathcal{P}) S^\dagger_{n_i} q_s]$. We took the jet directions to be n_1 and n_2, rather than n and $\bar n$, to emphasize that the soft operator is sensitive to the relative directions of the jets. The functions S_i shown in Table I are defined by the matrix element of this type of operator,

$$S_i(n_1\cdot k, n_1\cdot r, n_2\cdot q,) \equiv \langle 0|(\bar q_s S_{n_1})_{n_1\cdot r}\Gamma_i^{(1)}(S^\dagger_{n_2} q_s)_{n_2\cdot q} \times (\bar q_s S_{n_2})_{n_1\cdot k}\Gamma_i^{(2)}(S^\dagger_{n_1} h_v)|B(v)\rangle, \tag{51}$$

where i runs over color, Dirac, and flavor structures. To count the factors of π in these amplitudes, note that the hard-collinear contractions give g^4, and that the matrix element of the resulting four-quark operator, $\langle 0|(\bar q \ldots q)\times(\bar q \ldots b_v)|B\rangle$, is suppressed by $1/(4\pi)^2$ relative to $\langle 0|(\bar q \ldots b_v)|B\rangle$. (The four-quark operator has an extra loop with no extra couplings.) This demonstrates that nonperturbative complex contributions first occur at order $[\alpha_s(\mu_i)^2/\pi](\Lambda/m_b)$, i.e., suppressed by $[\alpha_s(\mu_i)/\pi]\times(\Lambda/m_b)$ compared to the leading amplitudes. The phases arising from the type of matrix element shown in Eq. (51) play a crucial role in explaining the observed strong phases which arise in color suppressed decays [3]. Their resulting operators predict the equality of amplitudes and strong phases between decays involving D and D^* mesons and have been confirmed in the data [39]. This type of diagram also has long-distance contributions of the same order, which arise from time-ordered products in $\mathrm{SCET_{II}}$ and can also be complex. To see this note that the hard-collinear quark propagator in Fig. 3(a) could also be on shell [i.e., have $\mathcal{O}(\Lambda^2)$ virtuality], in which case it would remain open until the matrix element is taken at the low scale. By opening that line we see that this contribution corresponds to the time-ordered product of a four-quark operator and a six-quark operator, both of which are generated when matching onto $\mathrm{SCET_{II}}$. A long-distance part is the same order in $\alpha_s(\mu_i)$ and does not change our conclusions about these terms. In Fig. 3(b) we show a nonannihilation contribution to $\hat A^{(1)}_{\rm rest}$ which is of order $\alpha_s(\mu_i)\Lambda/m_b$. This term is generated by the time-ordered product of $Q^{(1)}$, an insertion of the n_1-collinear $\mathcal{L}^{(1)}_{\xi q}$, and an operator with n_2-collinear quarks and usoft gluons,

$$\mathcal{L}^{(2)}_{\xi\xi} = (\bar\xi_n W) Y^\dagger_{n_2} i\not{D}^\perp_{\rm us} \frac{1}{in_1\cdot D_{\rm us}} i\not{D}^\perp_{\rm us} Y_{n_2} \frac{\not{n}_1}{2}\bar{\mathcal{P}}(W^\dagger \xi_n). \tag{52}$$

VI. APPLICATIONS AND CONCLUSION

A. Phenomenological implications

To understand the implications of the experimental data, it is crucial to know which contributions to the $B\to M_1M_2$ amplitudes can be complex. The best sensitivity to non-SM physics is via interference phenomena, where new interactions enter linearly (instead of quadratically), such as CP-violating observables. The sensitivity to such effects depends on how well we understand the dominant and subdominant SM amplitudes, including their strong phases. The existence of strong phases in B decays is experimentally well established (e.g., the $B\to D\pi$ and $B\to\pi\pi$ rates, the CP asymmetry $A_{K^+\pi^-}$, the transversity analysis in $B\to J/\psi K^*$, etc.).

One example of how strong phase information can be useful is the method for determining γ from $B\to\pi\pi$ proposed in Ref. [40]. The method uses isospin, the factorization prediction that $\mathrm{Im}(C/T)\sim\mathcal{O}(\alpha_s(m_b),\Lambda/m_b)$, and does not require data on the poorly measured direct CP asymmetry $C_{\pi^0\pi^0}$.[5] The phases in $A^{(0)}$ at $\alpha_s(m_b)\alpha_s(\mu_i)$ are calculable and partially known [2,41]. The current $B\to\pi\pi$ data are in mild conflict (at the $\sim 2\sigma$ level) with the SM CKM fit [42]. More precise measurements are needed to understand how well the theoretical expectations are satisfied, and to decipher whether there might be a hint for new physics. Obviously further information about power corrections in $\mathrm{Im}(C/T)$ could help to clarify the situation.

In all factorization-based approaches to charmless B decays, several parameters are fit from the data or are allowed to vary in certain ranges. The choice and ranges of these parameters should be determined by the power counting. This motivated keeping the charm penguin amplitudes, $A_{c\bar c}$, as free parameters in SCET [5], as was done earlier in Ref. [12]. In the BBNS approach these are argued to be factorizable [2]. A fit to the data using this parametrization found large power suppressed effects [43] including annihilation amplitudes, which might be interpreted as a breakdown of the Λ/m_b expansion. In QCD sum rules, the annihilation amplitude was found to be of the expected magnitude and to have a sizable strong phase [44], but a distinction between the terms we identify as real local annihilation and complex time-ordered product annihilation was not made.

[5]Here C and T are isospin amplitudes defined in the t convention, where λ_t is eliminated from the amplitudes in favor of λ_c and λ_u.

Channels like $B \to K\pi$ and $B \to K\bar{K}$ are sensitive to new physics, but by the same token are dominated by penguin amplitudes, which can have charm penguin, annihilation, and other standard model contributions. Since there are possible large nonperturbative c-loop contributions in $A_{c\bar{c}}$ that have the same $SU(3)$ flavor transformation properties as annihilation terms, they cannot be easily distinguished by simple fits to the data. However, in a systematic analysis based on SCET these correspond to different operators' matrix elements, so it is possible to disentangle the various contributions and determine their expected size. The factorization theorems for annihilation amplitudes derived here only involve distributions that already occurred at leading order. This means that we can compare the size of annihilation amplitudes to experimental data without further ambiguities from additional hadronic parameters. We take up this comparison in Sec. VI B below.

As an explicit example of how to assemble our results in Secs. III and IV, we derive the local annihilation amplitude for $\bar{B}^0 \to K^-\pi^+$. From Table II we can read off the result for this channel, $H(x,y) = -a_4^s(x,y) - a_8^s(x,y)$, and from Table IV, $H_{\chi 1} = -a_1^\chi(x,y) + 1/2 a_5^\chi(x,y)$ and $H_{\chi 2} = a_2^\chi(x,y) - 1/2 a_6^\chi(x,y)$. With the lowest order matching results in Eqs. (24) and (38) we can set $a_8 = 0$ and $a_{4u} = a_{4c}$, which inserted into Eqs. (23) and (43) gives

$$
\begin{aligned}
A^{(1)}_{\rm Lann}(K^-\pi^+) &= \frac{G_F f_B f_\pi f_K}{\sqrt{2}}(\lambda_c^{(s)} + \lambda_u^{(s)}) \int dx dy a_{4u}(x,y)\phi^\pi(y)\phi^K(x) = \frac{G_F f_B f_\pi f_K}{\sqrt{2}}(\lambda_c^{(s)} + \lambda_u^{(s)})\beta_{4u}^{\pi K},\\
A^{(2)}_{\rm Lann}(K^-\pi^+) &= \frac{G_F f_B f_\pi f_K}{6\sqrt{2}}(\lambda_c^{(s)} + \lambda_u^{(s)}) \int dx dy \Bigg[\frac{\mu_\pi}{m_b}\Big\{a_1^\chi(x,y) - \frac{1}{2}a_5^\chi(x,y)\Big\}\phi_{pp}^\pi(y)\phi^K(x)\\
&\quad - \frac{\mu_K}{m_b}\Big\{a_2^\chi(x,y) - \frac{1}{2}a_6^\chi(x,y)\Big\}\phi^\pi(y)\phi_{pp}^K(x)\Bigg]\\
&= \frac{G_F f_B f_\pi f_K}{\sqrt{2}}(\lambda_c^{(s)} + \lambda_u^{(s)})\Bigg[\frac{\mu_\pi}{m_b}\Big\{\beta_{\chi 1}^{\pi K} - \frac{1}{2}\beta_{\chi 5}^{\pi K}\Big\} - \frac{\mu_K}{m_b}\Big\{\beta_{\chi 2}^{\pi K} - \frac{1}{2}\beta_{\chi 6}^{\pi K}\Big\}\Bigg].
\end{aligned}
\tag{53}
$$

Thus, both the leading order annihilation amplitude $A^{(1)}_{\rm Lann}$ and the chirally enhanced annihilation amplitude $A^{(2)}_{\rm Lann}$ are determined by the β's defined in Eqs. (26) and (44). Other $K\pi$ channels have similar expressions with different Clebsch-Gordan coefficients. To the local annihilation contributions we must add the hard-collinear annihilation terms computed in Ref. [19], $A^{(1{\rm ann})}_{\text{hard-collin}}$, since they are the same order in α_s and $1/m_b$ as the $A^{(1)}_{\rm Lann}$ terms. To see explicitly what the β's involve, we insert the $\mathcal{O}(\alpha_s)$ values of $a_{3u}(x,y)$, $a_1^\chi(x,y)$, and $a_2^\chi(x,y)$ to give

$$
\begin{aligned}
A_{\rm Lann}(K^-\pi^+) = &-\frac{G_F f_B f_{M_1} f_{M_2}}{\sqrt{2}}(\lambda_c^{(s)} + \lambda_u^{(s)})\frac{4\pi\alpha_s(\mu_h)}{9}\Bigg\{\Big(\frac{C_9}{6} - \frac{C_3}{3}\Big)\Big[\langle\bar{x}^{-2}\rangle^K\langle y^{-1}\rangle^\pi - \langle[y(x\bar{y}-1)]^{-1}\rangle^{\pi K}\\
&+ d(\mu_-)\phi_K'(1)\langle y^{-1}\rangle^\pi\Big] - \frac{2\mu_\pi}{3m_b}\Big(C_6 - \frac{C_8}{2} + \frac{C_5}{3} - \frac{C_7}{6}\Big)\Big[\langle y^{-2}\bar{y}^{-1}\rangle_{pp}^\pi(\langle\bar{x}^{-2}\rangle^K + \langle\bar{x}^{-1}\rangle^K) + d_1(\mu_-)\\
&\times\phi_K'(1)\langle y^{-2}\bar{y}^{-1}\rangle_{pp}^\pi - d_2(\mu_+)\phi_\pi'(0)(\langle\bar{x}^{-2}\rangle^K + \langle\bar{x}^{-1}\rangle^K) - d_3(\mu_\pm)\phi_K'(1)\phi_\pi'(0)\Big]\\
&- \frac{2\mu_\pi}{3m_b}\Big(\frac{C_5}{3} - \frac{C_7}{6}\Big)\langle[(1-x\bar{y})\bar{x}y^2]^{-1}\rangle_{pp}^{\pi K} + \frac{2\mu_K}{3m_b}\Big(\frac{C_5}{3} - \frac{C_7}{6}\Big)\langle[(1-x\bar{y})\bar{x}^2 y]^{-1}\rangle_{pp}^{K\pi}\\
&- \frac{2\mu_K}{3m_b}\Big(C_6 - \frac{C_8}{2} + \frac{C_5}{3} - \frac{C_7}{6}\Big)\Big[(\langle y^{-2}\rangle^\pi + \langle y^{-1}\rangle^\pi)\langle x^{-1}\bar{x}^{-2}\rangle_{pp}^K - d_1(\mu_+)\phi_\pi'(0)\langle\bar{x}^{-2}x^{-1}\rangle_{pp}^K\\
&+ d_2(\mu_-)\phi_K'(1)(\langle y^{-2}\rangle^\pi + \langle y^{-1}\rangle^\pi) - d_3(\mu_\pm)\phi_\pi'(0)\phi_K'(1)\Big]\Bigg\}.
\end{aligned}
\tag{54}
$$

Here results for the convolutions denoted by brackets $\langle\cdots\rangle$ can be found in Eqs. (29), (33), (46), and (47) in the minimal subtraction scheme. Results for other channels can be assembled in a similar fashion. Corrections to $A_{\rm Lann} + A^{(1{\rm ann})}_{\text{hard-collin}}$ are suppressed by $\mathcal{O}[\alpha_s^2(\mu_i)/(\pi\alpha_s(m_b))]$, while we caution that additional $\alpha_s(\mu_h)\Lambda/m_b$ terms without a μ_π or μ_K will be present in Eq. (54). In the next subsection we derive results for all of these channels using a simple model for the distribution functions, and study numerically the size of the annihilation amplitudes.

Annihilation contributions have been claimed to play important roles in several observables [7,8,10,11,31], in particular, in generating large strong phases in $B \to K\pi$ decays [7,8]. The $B \to \pi\pi$ and $K\pi$ data indicate that the latter decays are dominated by penguin amplitudes, and the pattern of rates and CP asymmetries is not in good agreement with some predictions. In particular, it is not easy in the BBNS analysis to accommodate the measured CP asymmetry, $A_{K^+\pi^-} = -0.108 \pm 0.017$ [45], except in the S3 and S4 models of Ref. [11]. In these models the annihilation contributions are included by using asymptotic

distributions, and divergent integrals are parametrized as $\int_0^1 dx/x \to X_A$ and $\int_0^1 dx \ln x/x \to -X_A^2/2$, with $X_A = (1 + \varrho_A e^{i\varphi_A}) \ln(m_B/500\ \mathrm{MeV})$. Model S3 postulates $\varrho_A = 1$, $\varphi_A = -45°$ for all final states, while in the S4 scenario $\varrho_A = 1$ and $\varphi_A = -55°, -20°, -70°$ for the PP, PV, VP channels, respectively. Thus

$$\begin{aligned} &S3\text{: } X_A = 4.0 - 1.7i, \\ &S4\text{: } X_A = \{3.7 - 1.9i, 4.6 - 0.8i, 3.2 - 2.2i\}. \end{aligned} \tag{55}$$

In addition, $\alpha_s(\mu)$ and the Wilson coefficients are evaluated at the μ_i intermediate scale [11].

Our result for the factorization of annihilation contributions derived in Sec. III constrains models of annihilation. Equation (23) gives a well-defined and real amplitude at leading order, which depends on twist-2 distributions, ϕ_M. It does not involve model parameters ϱ_A and φ_A. For $A^{(1)}_{\mathrm{Lann}}$, using Eq. (29) and the asymptotic form of the meson distributions, we find a correspondence

$$\text{“}X_A\text{”} = 1 + \int_0^1 dx \frac{\phi_\pi(x)}{6(x^2)_\phi} = \ln\!\left(\frac{m_b}{\mu_+}\right). \tag{56}$$

Clearly, X_A is real. The asymptotic distributions $\sim 6x(1-x)$ are more accurate for large scales, and at the matching scale where $\mu_+ \sim m_b$, X_A is not enhanced by a large logarithm. This matching scale μ_+ should not be decreased below m_b since $\mu_+ \sim m_b$ is already the correct scale for collinear modes with $p^+ \sim m_b$. We estimate $|X_A| \lesssim 1$. Thus, the modeling of annihilation contributions with complex X_A in the BBNS approach (including the phenomenologically favored S3 and S4 scenarios) is in conflict with the heavy quark limit, and should be constrained to give smaller real X_A's.

In the KLS [7] treatment of annihilation, complex amplitudes are generated from dynamics at the intermediate scale from the $i\epsilon$ in propagators. The MS factorization used in the derivation of our annihilation amplitudes demonstrates that including the $i\epsilon$ term in collinear factorization would induce a double counting. Thus we expect such contributions to physical strong phases to be realized by operators with soft exchange that occur at higher order in Λ/m_b, and therefore to be small.

Annihilation contributions were also argued to play an important role in explaining the large transverse polarization fraction in $B \to \phi K^*$ [31]. It was shown that factorization implies $R_T = \mathcal{O}(1/m_b^2)$, where R_T denotes the transverse polarization fraction [31]. Subsequently, it was shown using SCET that R_T is power suppressed unless a long-distance charm penguin amplitude $A_{c\bar{c}}$ spoils this result [5,23]. Experimentally, one finds $R_T(B \to \phi K^*) \approx 0.5$ [45], while $R_T(B \to \rho\rho)$ is at the few percent level. It has been argued that the large $R_T(B \to \phi K^*)$ may provide a hint of new physics in the $b \to s\bar{s}s$ channel. In Ref. [31] it was suggested that standard model annihilation contributions may account for the observed large value of $R_T(B \to \phi K^*)$. Our analysis in Sec. IV agrees with [31] in that annihilation contributions to the transverse polarization amplitude at first order in α_s are suppressed by not one, but two powers of Λ/m_b. However, we do not find a numerical enhancement of these terms [which in [31] is partly due to the large sensitivity of the $(2X_A - 3)(1 - X_A)$ function to ϱ_A in the BBNS parametrization]. The operators in Eq. (36) give rise to transverse polarization, but since MS factorization renders the naively divergent convolutions finite, these power suppressed amplitudes do not receive sizable enhancements. Although we have not derived explicit results for the $B \to \phi K^*$ annihilation amplitudes (since ϕ is an isosinglet), our results make it unlikely that local annihilation can explain the $R_T(B \to \phi K^*)$ data. We have not explored whether the time-ordered products at $\mathcal{O}(\alpha_s^2(\mu_i)\Lambda/m_b)$ could give rise to transverse polarization, and it would be interesting to do so.

B. Annihilation amplitudes with simple models for $\phi^M(x)$ and $\phi^M_{pp}(x)$

In this section we derive numerical results for the local annihilation amplitudes in various channels using a simple model for the distributions. It is convenient to write the $\Delta S = 0$ local annihilation amplitude as

$$\begin{aligned} A_{\mathrm{Lann}}(\bar{B} \to M_1 M_2) = -\frac{G_F f_B f_{M_1} f_{M_2}}{\sqrt{2}} \Big\{ & \lambda_u^{(d)} h_u(\bar{B} \to M_1 M_2) \\ & + \lambda_c^{(d)} h_c(\bar{B} \to M_1 M_2) \\ & + (\lambda_u^{(d)} + \lambda_c^{(d)}) \Big[\frac{\mu_{M_1}}{m_b} h_{\chi 1}(\bar{B} \to M_1 M_2) \\ & + \frac{\mu_{M_2}}{m_b} h_{\chi 2}(\bar{B} \to M_1 M_2) \Big] \Big\}. \end{aligned} \tag{57}$$

For $\Delta S = 1$ decays we replace $\lambda_{u,c}^{(d)} \to \lambda_{u,c}^{(s)}$. The coefficients h_u, h_c, $h_{\chi 1}$, and $h_{\chi 2}$ are equal to linear combinations of β_{iu}, β_{ic}, $\beta_{\chi 1}$, $\beta_{\chi 2}$, $\beta_{\chi 5}$, and $\beta_{\chi 6}$ with Clebsch-Gordan coefficients determined from Tables II, III, IV, and V. The combinations are simply determined by the replacements

$$\begin{aligned} h_u &= (H(x,y) \ \text{ with } \tilde{a}_i^{d,s}(x,y) \to \beta_{iu}^{M_1 M_2}, \tilde{a}_i^{d,s}(y,x) \to \beta_{iu}^{M_2 M_1}), \\ h_c &= (H(x,y) \ \text{ with } \tilde{a}_i^{d,s}(x,y) \to \beta_{ic}^{M_1 M_2}, \tilde{a}_i^{d,s}(y,x) \to \beta_{ic}^{M_2 M_1}), \\ h_{\chi 1} &= (H_{\chi 1}(x,y) \ \text{ with } a_{1,5}^{\chi}(x,y) \to \beta_{\chi 1, \chi 5}), \\ h_{\chi 2} &= (H_{\chi 2}(x,y) \ \text{ with } a_{2,6}^{\chi}(x,y) \to \beta_{\chi 2, \chi 6}). \end{aligned} \tag{58}$$

For the coefficients $a_{3u,3c,4u,4c,7,8}$ and the a_i^{χ}'s, the $\mathcal{O}(\alpha_s^2 C_{1,2})$ matching corrections could be comparable numerically to the $\mathcal{O}(\alpha_s C_{3-10})$ corrections considered here. This should be kept in mind when examining numbers quoted below for the corresponding β's.

Results for the coefficients β_{iu}, β_{ic}, and $\beta_{\chi i}$ can be found in Eqs. (26) and (44). To derive numerical results we need to model the meson distribution functions. The C_i's are given in Eq. (3). We use

$$\alpha_s(\mu_h) = 0.22, \qquad \mu_\pi(\mu_h) = 2.3 \text{ GeV},$$
$$\mu_K(\mu_h) = 2.7 \text{ GeV}, \qquad f_K = 0.16 \text{ GeV},$$
$$f_\pi = 0.13 \text{ GeV}, \qquad f_B = 0.22 \text{ GeV}, \tag{59}$$

where $\mu_h = m_b = 4.7$ GeV, and f_B comes from a recent lattice determination [46]. For the ϕ's we take simple models with parameters a_i^M and a_{ipp}^M which we consider specified at the high scale μ_h,

$$\begin{aligned}\phi^M(x) &= 6x(1-x)[1 + a_1^M(6x-3) \\ &\quad + 6a_2^M(1 - 5x + 5x^2)], \\ \phi_{pp}^P(x) &= 6x(1-x)[1 + a_{1pp}^P(6x-3) \\ &\quad + 6a_{2pp}^P(1 - 5x + 5x^2)].\end{aligned} \tag{60}$$

Based on recent lattice data for moments of the π and K distributions [47], we take $a_2^{\pi,K} = 0.2 \pm 0.2$, where the lattice error was doubled to give some estimate for higher moments. For the π we set $a_1^\pi = a_{1pp}^\pi = 0$, while for the K we use [47] $a_1^K = 0.05 \pm 0.02$. We also take $w_{3\pi,K} = -3 \pm 1$, $a_{2pp}^{\pi,K} = 0 \pm 0.4$, and $a_{1pp}^K = 0.0 \pm 0.2$. Note that the range for our parameters is similar to those used in the BBNS models [10,11] and light-cone sum rules [48]. Since the uncertainties in the model parameters are large and not significantly affected by variation of the $\mu_\pm$ scales, we keep these fixed at m_b, where the logs in the $d_i(\mu_\pm)$ terms drop out and the constant under the logs are neglected. A scan over models with parameters in these limits gives predictions for the annihilation coefficients. For the $\bar{B} \to K\pi$ channels we find

$$\begin{aligned}&\beta_{2u}^{\pi K} = 1.8 \pm 1.2, && \beta_{4u}^{\pi K} = \beta_{4c}^{\pi K} = -0.15 \pm 0.10, \\ &\beta_{2c}^{\pi K} = 0.14 \pm 0.09, && \beta_{hc1}^{\pi K} = 0.09 \pm 0.33, \\ &\beta_{hc2}^{\pi K} = -0.29 \pm 0.09, && \beta_{hc3}^{\pi K} = -0.012 \pm 0.002, \\ &\beta_{hc4}^{\pi K} = 0.002 \pm 0.01, && \beta_{\chi 1}^{\pi K} = 0.0 \pm 6.5, \\ &\beta_{\chi 2}^{\pi K} = 0.0 \pm 5.8, && \beta_{\chi 5}^{\pi K} = 0.0 \pm 0.094, \\ &\beta_{\chi 6}^{\pi K} = 0.0 \pm 0.11.\end{aligned} \tag{61}$$

Using these numbers we can compare the size of the local annihilation amplitudes to the $\bar{B} \to K^-\pi^+$ data,

$$\begin{aligned}R_A(K^-\pi^+) &= \frac{|A_{\text{Lann}}^{(1)}(K^-\pi^+) + A_{\text{Lann}}^{(2)}(K^-\pi^+)|}{|A_{\text{Expt. Penguin}}(K\pi)|} \\ &= 0.11 \pm 0.09, \\ R_A(\bar{K}^0\pi^-) &= \frac{|A_{\text{Lann}}^{(1)}(\bar{K}^0\pi^-) + A_{\text{Lann}}^{(2)}(\bar{K}^0\pi^-)|}{|A_{\text{Expt. Penguin}}(K\pi)|} \\ &= 0.12 \pm 0.09.\end{aligned} \tag{62}$$

For the numerator we did a Gaussian scan using the values from Eq. (61), and determined the error by the standard deviation. For the denominator we used the experimental penguin amplitude determined by a fit to the $B \to K\pi$ data in Ref. [6]. Numerical results for annihilation amplitudes with three-body distribution functions were considered in Ref. [19]. Although they are similar in size to $A_{\text{Lann}}^{(1)}$, they cause only a $\sim$10% change in the value of $R_A(K^-\pi^+)$ in Eq. (62). The values of R_A indicate that a fairly small portion of the measured penguin amplitude is from annihilation. We do not quote values for the ratio $A_{\text{Lann}}^{(2)}/A_{\text{Lann}}^{(1)}$, since the numerator and denominator can each vanish and the parametric uncertainties are large. For typical values of the parameters in the $K\pi$ channels, we find that the $A_{\text{Lann}}^{(2)}$ is comparable or even larger than $A_{\text{Lann}}^{(1)}$ in agreement with Ref. [10]. The size of the annihilation amplitudes in Eq. (62) are consistent with our expectation for these power corrections. For $B \to \bar{K}K$ we find

$$\begin{aligned}&\beta_{1u}^{\bar{K}K} = -9.6 \pm 6.2, && \beta_{2u}^{\bar{K}K} = 1.7 \pm 1.1, \\ &\beta_{3u}^{\bar{K}K} = \beta_{3c}^{\bar{K}K} = 0.63 \pm 0.37, \\ &\beta_{4u}^{\bar{K}K} = \beta_{4c}^{\bar{K}K} = -0.14 \pm 0.09, \\ &\beta_{1c}^{\bar{K}K} = -0.03 \pm 0.02, && \beta_{2c}^{\bar{K}K} = 0.13 \pm 0.08, \\ &\beta_{3u}^{K\bar{K}} = \beta_{3c}^{K\bar{K}} = 0.63 \pm 0.37, && \beta_{\chi 1}^{\bar{K}K} = 0.0 \pm 6.5, \\ &\beta_{\chi 2}^{\bar{K}K} = 0.0 \pm 5.5 && \beta_{\chi 5}^{\bar{K}K} = 0.0 \pm 0.095, \\ &\beta_{\chi 6}^{\bar{K}K} = 0.0 \pm 0.11.\end{aligned} \tag{63}$$

Using these results to determine the $\lambda_c^{(d)}$ annihilation contributions to $B \to \bar{K}K$ and comparing this to the experimental penguin amplitude from Ref. [6] gives

$$\begin{aligned}R_A(K^-K^0) &= \frac{|A_{\text{Lann}}^{(1)}(K^-K^0) + A_{\text{Lann}}^{(2)}(K^-K^0)|}{|A_{\text{Expt. Penguin}}(\bar{K}K)|} \\ &= 0.15 \pm 0.11.\end{aligned} \tag{64}$$

The size of the ratios in Eqs. (62) and (64) are similar and consistent with the expected size of power corrections.

C. Conclusions

In summary, we exhibited how a new factorization in SCET renders the annihilation and "chirally enhanced" annihilation contributions finite in charmless nonleptonic $B \to M_1M_2$ decays to nonisosinglet mesons. We constructed a complete basis of SCET_II operators for local annihilation contributions as well as factorization theorems valid to all orders in α_s. By matching the full QCD diagrams onto SCET_II operators, we showed that their matrix elements are real at leading order in Λ/m_b and $\alpha_s(m_b)$. The lowest order annihilation contributions depend on f_B and a modified type of twist-2 distributions $\phi^{M_{1,2}}$ with dependence on rapidity cutoffs. Chirally enhanced local annihilation contributions depend, in addition, on modified distributions $\phi_{pp}^{M_{1,2}}$. The annihilation contributions can only have an unsuppressed complex part at $\mathcal{O}(\Lambda/m_b)$ if perturbation theory at the intermediate scale, $\sqrt{\Lambda m_b}$, breaks down.

In the previous literature models for the power suppressed annihilation corrections were often found to give enhanced contributions with large strong phases, and such assumptions have been important in some fits to the data. By considering all power suppressed amplitudes not involving charm loops, we proved that complex annihilation contributions are parametrically suppressed by at least $\alpha_s(\sqrt{\Lambda m_b})\Lambda/m_b$ compared to the leading amplitude. From our factorization theorem we found that annihilation contributes $(11 \pm 9)\%$ of the penguin amplitude in $\bar{B}^0 \to K^-\pi^+$, $(12 \pm 9)\%$ in $B^- \to \bar{K}^0\pi^-$, and $(15 \pm 11)\%$ in $B^- \to K^-K^0$. We anticipate that our results will guide future fits to the vast amount of data on charmless B decays, and yield a better understanding of what these data mean.

ACKNOWLEDGMENTS

This work was supported in part by the Director, Office of Science, Offices of High Energy and Nuclear Physics of the U.S. Department of Energy under the Contract No. DE-AC02-05CH11231 (Z. L.), the Cooperative Research Agreement No. DOE-FC02-94ER40818 (C. A. and I. S.), and No. DOE-ER-40682-143 and No. DEAC02-6CH03000 (I. R.). I. S. was also supported in part by the DOE OJI program and by the Sloan Foundation.

APPENDIX: ZERO-BIN SUBTRACTIONS FOR A TWO-DIMENSIONAL DISTRIBUTION

In this appendix we derive a result for the action of the zero-bin subtractions on the integrand obtained from the chirally enhanced annihilation computation, shown in Eq. (47). Since the result involves a correlation in the x and y integrals, it cannot be read off from the results in Ref. [18]. It is convenient to write the momentum fraction factor coming from the off-shell b-quark propagator as $(1 - x\bar{y}) = (\bar{x} + y - \bar{x}y)$. Including the rapidity convergence factors [18], the integral we need is

$$I = \sum_{x\neq 1, y\neq 0} \int dx_r dy_r \frac{\phi_{pp}^{M_1}(y)\phi^{M_2}(x)}{(\bar{x} + y - \bar{x}y)\bar{x}y^2}\Theta_x\Theta_y \times |x(1-x)|^\epsilon |y(1-y)|^\epsilon \left(\frac{\mu_+\mu_-}{\bar{n}\cdot p_1 n\cdot p_2}\right)^{2\epsilon}, \quad \text{(A1)}$$

where $\Theta_x = \theta(x)\theta(1-x)$. To determine the subtraction terms we must look at the singular behavior as we scale towards the $x = 1$ and $y = 0$ bins, which we do by taking $\bar{x} \sim \eta$ and $y \sim \eta$. In this limit the gluon and b quark in Fig. 2 become soft, and this region would be double counted without the zero-bin conditions. First consider the denominator,

$$\frac{1}{\bar{x} + y - \bar{x}y} = \frac{1}{(\bar{x} + y)} + \frac{\bar{x}y}{(\bar{x} + y)^2} + \ldots. \quad \text{(A2)}$$

In the first term the x and y dependence does not decouple, so we must consider them simultaneously. All terms beyond the first one produce finite integrals and are dropped in the minimal subtraction scheme. For the numerator in Eq. (A1) we use $\phi_{pp}^{M_1}(0) = \phi^{M_2}(1) = 0$ and expand

$$\begin{aligned}\phi_{pp}(y)\phi(x) &= -y\phi'_{pp}(0)\bar{x}\phi'(1) - \frac{y^2}{2}\phi''_{pp}(0)\bar{x}\phi'(1) \\ &\quad + y\phi'_{pp}(0)\frac{\bar{x}^2}{2}\phi''(1) + \ldots \\ &= y\phi'_{pp}(0)\sum_{n=1}^{\infty}\frac{(-\bar{x})^n}{n!}\phi^{(n)}(1) \\ &\quad - \frac{y^2}{2}\phi''_{pp}(0)\bar{x}\phi'(1) + \ldots. \end{aligned} \quad \text{(A3)}$$

In the term on the second to last line we have identified all terms which remain singular when multiplied by $1/[\bar{x}y^2(\bar{x} + y)]$. This term is equal to $y\phi'_{pp}(0)\phi(x)$. Taken together with the expansion of $\Theta_x\Theta_y$ we therefore find that the required minimal subtraction is

$$\frac{y\phi_{pp}^{M_1\prime}(0)\phi^{M_2}(x)}{(\bar{x} + y)\bar{x}y^2}\Theta_x\theta(y). \quad \text{(A4)}$$

Following Ref. [18] we use this to convert Eq. (A1) into an integral that includes the $x = 1$ and $y = 0$ regions,

$$\begin{aligned} I &= \int_0^1 dx \int_0^1 dy\left[\frac{\phi_{pp}^{M_1}(y)\phi^{M_2}(x)}{(\bar{x} + y - \bar{x}y)\bar{x}y^2} - \frac{y\phi_{pp}^{M_1\prime}(0)\phi^{M_2}(x)}{(\bar{x} + y)\bar{x}y^2}\right] \\ &\quad - \int_0^1 dx \int_1^\infty dy \frac{y\phi_{pp}^{M_1\prime}(0)\phi^{M_2}(x)}{(\bar{x} + y)\bar{x}y^2} x^\epsilon(1-x)^\epsilon y^\epsilon(y-1)^\epsilon\left(\frac{\mu_+\mu_-}{\bar{n}\cdot p_1 n\cdot p_2}\right)^{2\epsilon} \\ &= \int_0^1 dx \frac{\phi^{M_2}(x)}{\bar{x}} \int_0^1 dy\left[\frac{\phi_{pp}^{M_1}(y)}{(\bar{x} + y - \bar{x}y)y^2} - \frac{\phi_{pp}^{M_1\prime}(0)}{(\bar{x} + y)y}\right] - \int_0^1 dx \int_1^\infty dy \frac{\phi_{pp}^{M_1\prime}(0)\phi^{M_2}(x)}{(\bar{x} + y)\bar{x}y} y^\epsilon(y-1)^\epsilon \\ &= \int_0^1 dx \frac{\phi^{M_2}(x)}{\bar{x}} \int_0^1 dy\left[\frac{\phi_{pp}^{M_1}(y)}{(\bar{x} + y - \bar{x}y)y^2} - \frac{\phi_{pp}^{M_1\prime}(0)}{(\bar{x} + y)y}\right] - \phi_{pp}^{M_1\prime}(0)\int_0^1 dx \frac{\phi^{M_2}(x)\ln(2-x)}{(1-x)^2}. \end{aligned} \quad \text{(A5)}$$

Here, in simplifying the term carrying the $y \to \infty$ limit, we noted that the integral is finite, and so it does not induce $\mu_\pm$ dependence in our subtraction scheme. This result for I was used in Eq. (47). For the asymptotic pion wave functions, $\phi^\pi(x) = 6x(1-x)$ and $\phi^\pi_{pp}(y) = 6y(1-y)$, we obtain $I = 36 + 6\pi^2 - 144\ln 2 = -4.60$. Note that the steps used here to derive the subtraction also give the correct result for cases where the x and y integrals factorize, such as an integrand $\phi(x)\phi(y)/(x^2y^2)$.

[1] C. W. Bauer, D. Pirjol, and I. W. Stewart, Phys. Rev. Lett. **87**, 201806 (2001).
[2] M. Beneke, G. Buchalla, M. Neubert, and C. T. Sachrajda, Phys. Rev. Lett. **83**, 1914 (1999); Nucl. Phys. **B591**, 313 (2000).
[3] S. Mantry, D. Pirjol, and I. W. Stewart, Phys. Rev. D **68**, 114009 (2003).
[4] J. g. Chay and C. Kim, Phys. Rev. D **68**, 071502 (2003); Nucl. Phys. **B680**, 302 (2004).
[5] C. W. Bauer, D. Pirjol, I. Z. Rothstein, and I. W. Stewart, Phys. Rev. D **70**, 054015 (2004).
[6] C. W. Bauer, I. Z. Rothstein, and I. W. Stewart, Phys. Rev. D **74**, 034010 (2006).
[7] Y. Y. Keum, H. n. Li, and A. I. Sanda, Phys. Lett. B **504**, 6 (2001).
[8] Y. Y. Keum, H. N. Li, and A. I. Sanda, Phys. Rev. D **63**, 054008 (2001).
[9] C. D. Lu, K. Ukai, and M. Z. Yang, Phys. Rev. D **63**, 074009 (2001).
[10] M. Beneke, G. Buchalla, M. Neubert, and C. T. Sachrajda, Nucl. Phys. **B606**, 245 (2001).
[11] M. Beneke and M. Neubert, Nucl. Phys. **B675**, 333 (2003).
[12] M. Ciuchini, E. Franco, G. Martinelli, and L. Silvestrini, Nucl. Phys. **B501**, 271 (1997); M. Ciuchini *et al.*, Phys. Lett. B **515**, 33 (2001).
[13] P. Colangelo, G. Nardulli, N. Paver, and Riazuddin, Z. Phys. C **45**, 575 (1990).
[14] H. n. Li, arXiv:hep-ph/0408232.
[15] T. Feldmann and T. Hurth, J. High Energy Phys. 11 (2004) 037.
[16] C. W. Bauer, S. Fleming, and M. E. Luke, Phys. Rev. D **63**, 014006 (2000); C. W. Bauer, S. Fleming, D. Pirjol, and I. W. Stewart, Phys. Rev. D **63**, 114020 (2001); C. W. Bauer and I. W. Stewart, Phys. Lett. B **516**, 134 (2001); C. W. Bauer, D. Pirjol, and I. W. Stewart, Phys. Rev. D **65**, 054022 (2002).
[17] J. Malcles, arXiv:hep-ph/0606083; Y. L. Wu and Y. F. Zhou, Phys. Rev. D **72**, 034037 (2005); A. J. Buras, R. Fleischer, S. Recksiegel, and F. Schwab, Nucl. Phys. **B697**, 133 (2004); C. W. Chiang, M. Gronau, J. L. Rosner, and D. A. Suprun, Phys. Rev. D **70**, 034020 (2004).
[18] A. V. Manohar and I. W. Stewart, Phys. Rev. D **76**, 074002 (2007).
[19] C. M. Arnesen, I. Z. Rothstein and I. W. Stewart, Phys. Lett. B **647**, 405 (2007).
[20] M. A. Shifman, A. I. Vainshtein, and V. I. Zakharov, Nucl. Phys. **B120**, 316 (1977).
[21] G. Buchalla, A. J. Buras, and M. E. Lautenbacher, Rev. Mod. Phys. **68**, 1125 (1996).
[22] A. J. Buras and L. Silvestrini, Nucl. Phys. **B569**, 3 (2000).
[23] A. R. Williamson and J. Zupan, Phys. Rev. D **74**, 014003 (2006); **74**, 039901(E) (2006).
[24] C. W. Bauer, S. Fleming, D. Pirjol, I. Z. Rothstein, and I. W. Stewart, Phys. Rev. D **66**, 014017 (2002).
[25] C. W. Bauer, D. Pirjol, I. Z. Rothstein, and I. W. Stewart, Phys. Rev. D **72**, 098502 (2005).
[26] M. Beneke, G. Buchalla, M. Neubert, and C. T. Sachrajda, Phys. Rev. D **72**, 098501 (2005).
[27] C. W. Bauer, D. Pirjol, and I. W. Stewart, Phys. Rev. D **67**, 071502 (2003).
[28] B. O. Lange and M. Neubert, Nucl. Phys. **B690**, 249 (2004); **B723**, 201(E) (2005).
[29] H. n. Li, Czech. J. Phys. **53**, 657 (2003) [Prog. Part. Nucl. Phys. **51**, 85 (2003)].
[30] C. W. Bauer, D. Pirjol, and I. W. Stewart, Phys. Rev. D **68**, 034021 (2003).
[31] A. L. Kagan, Phys. Lett. B **601**, 151 (2004).
[32] B. O. Lange, A. V. Manohar, and I. W. Stewart (unpublished).
[33] V. L. Chernyak and A. R. Zhitnitsky, Phys. Rep. **112**, 173 (1984).
[34] A. Hardmeier, E. Lunghi, D. Pirjol, and D. Wyler, Nucl. Phys. **B682**, 150 (2004).
[35] S. Wandzura and F. Wilczek, Phys. Lett. **72B**, 195 (1977).
[36] M. Beneke, A. P. Chapovsky, M. Diehl, and T. Feldmann, Nucl. Phys. **B643**, 431 (2002).
[37] M. Bander, D. Silverman, and A. Soni, Phys. Rev. Lett. **43**, 242 (1979).
[38] T. Becher and R. J. Hill, J. High Energy Phys. 10 (2004) 055.
[39] S. Mantry, D. Pirjol, and I. W. Stewart, AIP Conf. Proc. **722**, 141 (2004); D. Pirjol, arXiv:hep-ph/0411124.
[40] C. W. Bauer, I. Z. Rothstein, and I. W. Stewart, Phys. Rev. Lett. **94**, 231802 (2005).
[41] M. Beneke and S. Jager, Nucl. Phys. **B751**, 160 (2006).
[42] Y. Grossman, A. Hocker, Z. Ligeti, and D. Pirjol, Phys. Rev. D **72**, 094033 (2005).
[43] J. Charles *et al.* (CKMfitter Group), Eur. Phys. J. C **41**, 1 (2005).
[44] A. Khodjamirian, T. Mannel, M. Melcher, and B. Melic, Phys. Rev. D **72**, 094012 (2005).
[45] E. Barberio *et al.* (Heavy Flavor Averaging Group), arXiv:hep-ex/0603003, and updates at http://www.slac.stanford.edu/xorg/hfag/.
[46] A. Gray *et al.* (HPQCD Collaboration), Phys. Rev. Lett. **95**, 212001 (2005).
[47] V. M. Braun *et al.*, Phys. Rev. D **74**, 074501 (2006).
[48] P. Ball, V. M. Braun, and A. Lenz, J. High Energy Phys. 05 (2006) 004.